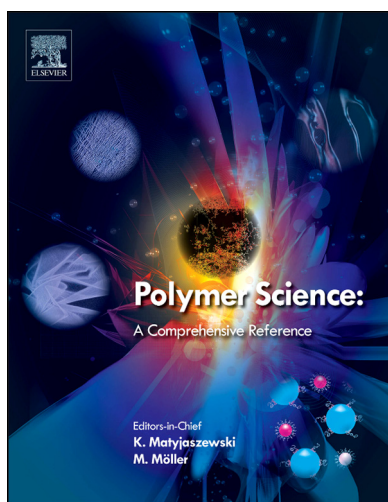


Provided for non-commercial research and educational use.  
Not for reproduction, distribution or commercial use.

This chapter was originally published in *Polymer Science: A Comprehensive Reference* published by Elsevier, and the attached copy is provided by Elsevier for the author's benefit and for the benefit of the author's institution, for non-commercial research and educational use including without limitation use in instruction at your institution, sending it to specific colleagues who you know, and providing a copy to your institution's administrator.



All other uses, reproduction and distribution, including without limitation commercial reprints, selling or licensing copies or access, or posting on open internet sites, your personal or institution's website or repository, are prohibited. For exceptions, permission may be sought for such use through Elsevier's permissions site at:

<http://www.elsevier.com/locate/permissionusematerial>

Pojman JA (2012) Frontal Polymerization. In: Matyjaszewski K and Möller M (eds.) *Polymer Science: A Comprehensive Reference*, Vol 4, pp. 957–980. Amsterdam: Elsevier BV.

© 2012 Elsevier B.V. All rights reserved.

## 4.38 Frontal Polymerization

JA Pojman, Louisiana State University, Baton Rouge, LA, USA

© 2012 Elsevier B.V. All rights reserved.

<b>4.38.1</b>	<b>What Is Frontal Polymerization?</b>	957
<b>4.38.2</b>	<b>Photofrontal Polymerization</b>	958
<b>4.38.3</b>	<b>Isothermal Frontal Polymerization</b>	958
<b>4.38.4</b>	<b>Cryogenic Fronts</b>	959
<b>4.38.5</b>	<b>Thermal Frontal Polymerization</b>	960
4.38.5.1	Origins	960
4.38.5.2	Attempts at Frontal Polymerization Reactors	960
4.38.5.3	Requirements for Frontal Polymerizations	960
4.38.5.4	Starting Fronts	961
4.38.5.5	Free-Radical Frontal Polymerization	961
4.38.5.6	Properties of Monomers	961
4.38.5.7	Frontal Polymerization in Solution	962
4.38.5.8	Temperature Profiles	962
4.38.5.9	Velocity Dependence on Initiator Concentration	963
4.38.5.10	Front Velocity as a Function of Temperature	963
4.38.5.11	The Effect of Type of Monomer and Functionality on Front Velocity	963
4.38.5.12	Solid Monomers	963
4.38.5.13	Effect of Pressure	965
4.38.5.14	Molecular Weight Distribution	966
4.38.5.15	Conversion	967
4.38.5.16	Interferences with Frontal Polymerization	968
4.38.5.16.1	Buoyancy-driven convection	968
4.38.5.16.2	Effect of surface tension-driven convection	969
4.38.5.16.3	Dispersion polymerization	970
4.38.5.16.4	Thermal instabilities	970
4.38.5.16.5	Effect of complex kinetics	971
4.38.5.16.6	Effect of bubbles	972
4.38.5.16.7	Effect of buoyancy	972
4.38.5.16.8	Three-dimensional frontal polymerization	972
4.38.5.17	The Effect of Fillers	973
4.38.5.18	Encapsulation of Initiators	973
4.38.5.19	Copolymerizations	973
4.38.5.20	Atom Transfer Radical Polymerization	973
4.38.5.21	Ring-Opening Metathesis Polymerization	973
4.38.5.22	Polyurethanes	974
4.38.5.23	Epoxy Curing	974
4.38.5.24	Binary Systems	974
4.38.5.25	Patents	975
4.38.5.26	Applications of Thermal Frontal Polymerization	975
4.38.5.26.1	Solventless processing	975
4.38.5.26.2	Energy savings	975
4.38.5.26.3	Rapid synthesis of materials	975
4.38.5.26.4	Preparation of hydrogels	975
4.38.5.26.5	Consolidation of stone	976
4.38.5.26.6	Autoclaveless curing of large composites	976
4.38.5.26.7	Cure-on-demand repair and adhesives	976
<b>4.38.6</b>	<b>Conclusions</b>	976
<b>References</b>		977

### 4.38.1 What Is Frontal Polymerization?

Frontal polymerization (FP) is a polymerization process in which polymerization occurs directionally in a localized reaction zone. There are three types of FP. The first is photofrontal

polymerization in which the front is driven by the continuous flux of radiation, usually UV light.<sup>1–7</sup> The second is isothermal frontal polymerization (IFP), which is based on the ‘gel effect’ to create a localized reaction zone to propagate slowly from a polymer seed. The last type is thermal frontal polymerization,

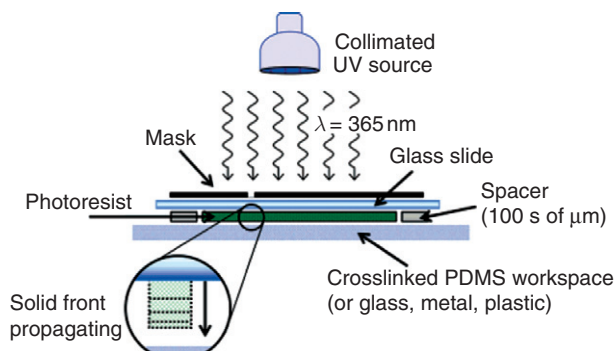


**Figure 1** A schematic of photofrontal polymerization method used to prepare microfluidic chips. Reprinted with permission from Cabral, J. T.; Hudson, S. D.; Harrison, C.; Douglas, J. F. *Langmuir* **2004**, *20*, 10020–10029.<sup>7</sup> Copyright 2004 American Chemical Society.

and it results from the coupling of thermal transport and the Arrhenius dependence of the reaction rate of an exothermic polymerization (Figure 1).

Photofrontal polymerization produces fronts whose positions depend logarithmically on time if the initiator continues to absorb light and linearly on time if the initiator is photobleached. It is limited in application to unfilled systems. IFP propagates on the order of  $1 \text{ cm day}^{-1}$  and only for total distances of about 1 cm. Thermal frontal polymerization has the widest range of velocities and types of chemistries that can be used.

#### 4.38.2 Photofrontal Polymerization

Photofrontal polymerization requires a continuous input of radiation, usually UV light, to create a propagating front. Koike *et al.*<sup>8</sup> and Ohtsuka and Koike<sup>9</sup> used photofrontal polymerization to create gradient optical materials (see next section). Briskman<sup>4</sup> and Righetti *et al.*<sup>10</sup> studied photopolymerization of acrylamide in weightlessness. The reaction mixture was composed of 18% aqueous solution of acrylamide with methylenebisacrylamide (0.46%), catalyst (tetramethylenediamide, 0.01%), and riboflavin ( $4.9 \times 10^{-4}\%$ ) as the initiator. The illumination was provided by a lamp with a maximum intensity at  $4450 \text{ \AA}$ . The experiment was performed in weightlessness (on the *Mir* space station) because buoyancy-driven convection was generated by the temperature and concentration gradients. In the absence of convection, the front position increased with the logarithm of illumination time. This reflects the exponential distribution of illumination in the sample caused by the absorption of the riboflavin.

Cabral *et al.*<sup>7</sup> developed a beautiful application of photofrontal polymerization for producing microfluidic chips. By illuminating through a glass plate in contact with a polymerizable resin, they created patterns that grew from the surface. If the polymer possessed the same absorption properties as the resin, then the front propagation was proportional to the logarithm of the dose (Figure 2). However, if the polymer absorbed more light than the resin, the position versus the logarithm of the dosage exhibits curvature. Warren *et al.*<sup>11</sup> analytically solved the phase-field model of the process.

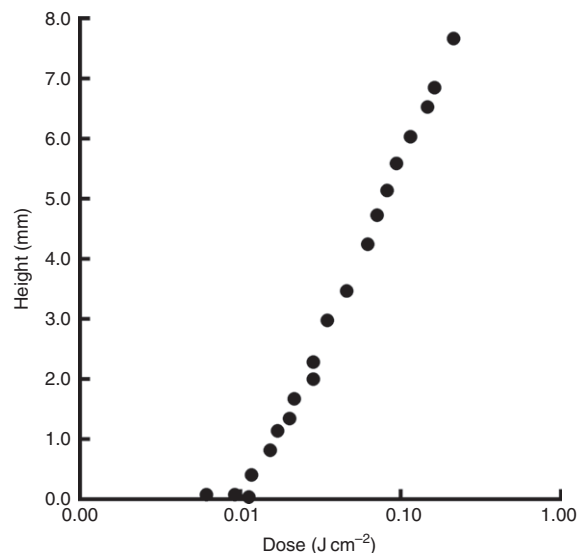


**Figure 2** 'Photoinvariant' polymerization: frontal kinetics of resist material whose transmission remains constant upon UV exposure. Adapted from Cabral, J. T.; Hudson, S. D.; Harrison, C.; Douglas, J. F. *Langmuir* **2004**, *20*, 10020–10029.<sup>7</sup>

If the photoinitiator is bleached, then a front with a constant velocity can be created. Terrones and Pearlstein<sup>5</sup> considered a model of free-radical photopolymerization with a photobleaching initiator. They derived an analytical expression for the front speed of the localized traveling wave

$$\text{Front speed} = \frac{\phi I_0}{C_{A,0}}$$

where  $\phi$ ,  $I_0$ , and  $C_{A,0}$  are the quantum yield of the photoinitiator, incident intensity, and photoinitiator concentration, respectively. They predicted and confirmed numerically that front velocity does not depend on the absorption coefficient of the initiator, as long as it is sufficiently large. However, the front profile is a function of the coefficient.

#### 4.38.3 Isothermal Frontal Polymerization

IFP is a slow process in which a localized polymerization propagates from a solid polymer piece into a solution of its monomer and a thermal radical initiator. The typical experiment requires placing a piece of high-molecular-weight poly (methyl methacrylate) (PMMA), the 'seed' in a solution of methyl methacrylate and azobisisobutyronitrile (AIBN). The monomer-initiator solution dissolves the polymer seed, creating a highly viscous 'gel' region (Figure 3). The initiator is decomposing throughout the system and initiating

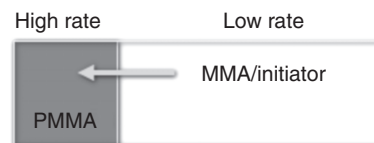


**Figure 3** Schematic of isothermal frontal polymerization.

polymerization but because of the Norrish–Trommsdorff effect (gel effect),<sup>12,13</sup> the rate of polymerization is higher in the gel region than that in the rest of the solution.

Koike *et al.*<sup>14</sup> first discovered this process and called it ‘interfacial gel polymerization’. He was interested in producing Gradient Refractive INdex (GRIN) optical materials.<sup>14–24</sup> GRIN materials are formed by dissolving a dopant in the monomer. Usually, the dopant possesses a higher refractive index than the polymer. As the front propagates, the dopant is partially incorporated in the polymer such that the dopant’s concentration increases in the bulk solution. If the front is performed in a cylindrical geometry with the polymer seed in the form of an annulus, then as the front propagates toward the center, the dopant concentration increases. When all the monomer finally polymerizes, a gradient in dopant concentration remains, which creates a gradient in refractive index. As we can observe in Figure 4, the flat disk of PMMA magnifies the letters because of the gradient of naphthalene that was created.

Such GRIN cylinders are useful because they can be used in optics.<sup>8,25</sup> More importantly, such cylinders can be drawn into GRIN optical fibers, which have a higher bandwidth for data transmission than step-index fibers.<sup>16,26</sup>

For all the work carried out on polymeric GRIN materials via interfacial gel polymerization in the 1980s and 1990s, little work was performed on the actual front propagation process. Golubev *et al.*<sup>27</sup> proposed a mechanism in 1992. Gromov and Frisch<sup>28</sup> proposed a mathematical model that was flawed. Ivanov *et al.* did work with IFP in 1997<sup>29</sup> and 2002.<sup>30</sup>

Lewis *et al.*<sup>31</sup> used the deflection of a sheet of laser light to measure the position of the front and measure the magnitude of the gradient between the monomer and polymer. In 2005, they confirmed the proposed mechanism of IFP from experiments and numerical modeling.<sup>32,33</sup> Evstratova *et al.*<sup>34</sup> confirmed that the process is indeed isothermal and there exists a minimum molecular weight required for the seed.

The fronts propagate a short distance because polymerization is occurring throughout the solution, and the fronts stop propagating when the monomer has bulk polymerized.



**Figure 4** An image of a GRIN lens created by a radically propagating front of methyl methacrylate polymerization from an annulus (1.5 cm) of PMMA. Naphthalene was initially present in the monomer and accumulated as the front propagated inward.

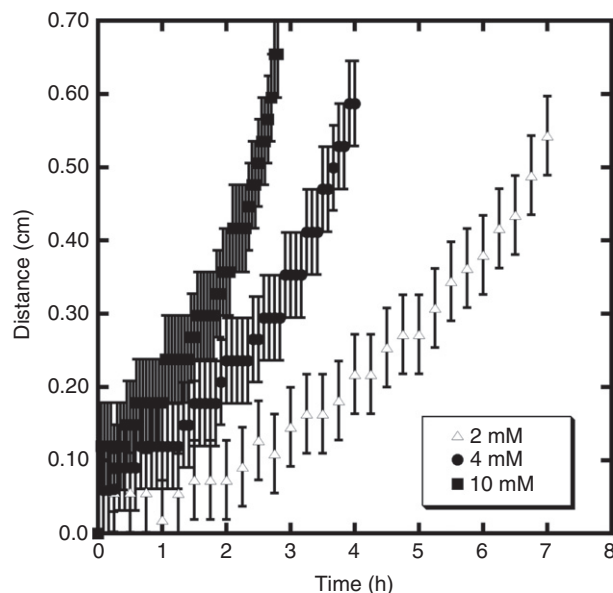


**Figure 5** The front position versus time for three different concentrations of AIBN in methyl methacrylate at 50 °C. Data courtesy of L. Lewis.

Because of the slow bulk polymerization, the front accelerates (Figure 5). This is because as the front propagates, it enters region of higher and higher conversion, which means it takes less time for the reaction in the front to reach high viscosity and thus high reaction rate. This is analogous to smoldering.<sup>35</sup> If a piece of paper is uniformly heated until smoldering commences and then a flame is ignited at one end, the flame will accelerate as it propagates. The temperature is analogous to the conversion in the polymer case.

Volpert and his colleagues have performed mathematical analysis of IFP,<sup>32,36,37</sup> and modeled how the nonuniform dopant distribution arises.<sup>38</sup>

Short front propagation is adequate for many applications, but propagation over greater distances than a centimeter is possible. Masere *et al.*<sup>39</sup> used IFP to create gradients of dyes over several centimeters by performing the experiments at 4 °C with triocetyl methyl ammonium persulfate.<sup>40</sup> Ivanov *et al.*<sup>29</sup> used a polymeric inhibitor that would not diffuse into the gel region but did prevent polymerization in the bulk solution.

IFP is a useful technique for producing gradient optical materials but it is limited to free-radical systems that exhibit the gel effect and whose polymers are soluble in their monomers.

#### 4.38.4 Cryogenic Fronts

A fascinating mode of frontal polymerization at temperatures of 77 K and below was developed at the Institute of Chemical Physics in Chernogolovka, Russia.<sup>41–47</sup> Many systems can be polymerized by this method, including acetaldehyde, formaldehyde, cyclopentadiene, and methyl methacrylate. Filled polymers, such as acetaldehyde and alumina, can also be prepared.<sup>48</sup>

The mechanism of propagation is via a non-Arrhenius mechanism. The monomer is frozen at a temperature from

4 to 77 K and then irradiated with gamma radiation. A monomer such as methyl methacrylate is cooled in liquid nitrogen or even liquid helium. Fronts are started by heating the surface. Temperature and density gradients arising in the reaction are responsible for further layer-by-layer disruption of the solid sample and creation of the surface on which the reaction continues. Because of this positive feedback between the solid-phase chemical reaction and the cracking of the frozen reagents, the polymerization proceeds in a layer-by-layer fashion and propagates through the entire sample as a front.

For example, epichlorohydrin can be rapidly cooled to 77 K and then irradiated with 680 kGy dose of gamma radiation.<sup>43</sup> A polymerization front with a velocity of  $1.3 \text{ cm s}^{-1}$  propagated after fracturing a small region of the sample. Cations formed by the irradiation were released by the cracking and a wave of polymerization resulted.

### 4.38.5 Thermal Frontal Polymerization

Thermal frontal polymerization is a process in which a localized reaction zone propagates from the coupling of thermal diffusion and the Arrhenius dependence of reaction rate of an exothermic polymerization. Thermal frontal polymerization was discovered at the Institute of Chemical Physics in Chernogolovka, Russia by Chechilo and Enikolopyan. They studied methyl methacrylate polymerization under 3500 atm pressure.<sup>49–52</sup> (We will consider later why these extreme conditions were used.) The literature from that Institute was reviewed in 1984.<sup>53</sup> Pojman<sup>54</sup> rediscovered what he called 'traveling fronts of polymerization' in 1991. Pojman *et al.*<sup>55</sup> reviewed the field in 1996. There have been other focused reviews.<sup>56,57</sup>

Thermal frontal polymerization is by far the most commonly studied form of FP, so we will henceforth refer to it as 'FP'. We will first consider the necessary conditions for FP and give an overview of the types of systems that have been studied.

#### 4.38.5.1 Origins

Thermal fronts have been used in a process discovered in 1967 by Merzhanov and co-workers<sup>58</sup> called self-propagating high-temperature synthesis (SHS) to prepare ceramics and intermetallic compounds.<sup>59–64</sup> Secondly, such fronts demonstrate a variety of dynamical behavior, including planar fronts, spin modes,<sup>65–68</sup> and chaotically propagating fronts.<sup>69</sup>

Chechilo *et al.*<sup>52</sup> were the first to study FP. They studied methyl methacrylate polymerization with benzoyl peroxide as the initiator. **Figure 1** is taken from their original data. They performed the reactions in closed metal reactors under pressure so they were unable to directly observe the front.

Chechilo and Enikolopyan<sup>51</sup> studied the effect of pressure on the velocity. Raising the pressure (up to 5000 atm) increased the velocity by effectively increasing the concentration of the monomer and increasing the polymerization rate constant. They reported that drops of polymer descended from the front, which underwent a convective breakdown. By increasing the pressure to >3500 atm, the instability was eliminated by possibly reducing the density difference between monomer and polymer and/or increasing the monomer/polymer viscosities.

In bulk polymerizations, as the viscosity increases, the rate of termination decreases causing autoacceleration, which is called the gel effect.<sup>12,13</sup> For a monomer such as methyl methacrylate, the gel effect can play a significant role in the kinetics. Davtyan *et al.*<sup>70</sup> examined the influence of the gel effect on the kinetics of radical polymerization in a front.

#### 4.38.5.2 Attempts at Frontal Polymerization Reactors

A natural early goal of FP researchers was to develop a reactor in which the monomer–initiator solution was pumped in such that the product would continuously flow out, without the input of heat. Attempts were made with reactors of cylindrical and spherical geometries. Zhizhin and Segal<sup>71</sup> performed a linear stability analysis of a reactor consisting of two concentric cylinders. A radial, axisymmetric front was supposed because the monomer/initiator would be pumped through the permeable inner cylinder. The viscous reacted polymer was supposed to flow out through the outer permeable cylinder. No buoyancy-driven convection was included. They found that if the resistance of the outer boundary was small, the front would become hydrodynamically unstable. They also considered a reactor with concentric spheres and found similar results.

Volpert and Volpert and their colleagues in Chernogolovka continued these analytical and numerical studies.<sup>72–77</sup> They found cases where the front would become unstable and develop spin modes and multiple steady states, which we will discuss in detail later. More numerical studies were performed for the spherical case by Solovyov *et al.*<sup>78</sup> They found that the front could be unstable, and chaotic oscillations with low frequency could result.

All the studies ignored the difference in density between reactants and product, which meant they could not consider how buoyancy-driven convection would affect the reactor performance. From work, we will consider shortly, convective instabilities are a major interference when using monomers that form molten polymer.

#### 4.38.5.3 Requirements for Frontal Polymerizations

For a system to support FP, it must have a low rate of reaction at the initial temperature but have a very high rate of reaction at a temperature between the initial temperature and the adiabatic reaction temperature. What we mean by the 'adiabatic reaction temperature' is the temperature reached if the reaction went to completion without heat loss. Clearly, the reaction must be exothermic. The essential criterion for FP is that the system must have an extremely low rate at the initial temperature but a high rate of reaction at the front temperature such that the rate of heat production exceeds the rate of heat loss. In other words, the system must react slowly or not at all at room temperature, have a large heat release, and have a high energy of activation. For free-radical polymerization, the peroxide or nitrile initiator provides the large activation energy. As we will discuss later, it is not possible to create a system that has a long pot life at room temperature and a rapid reaction at any arbitrary temperature if the system follows Arrhenius kinetics.

Thermal polymerization fronts can exhibit a wide range of interesting dynamical behavior.<sup>79,80</sup> Fronts do not have to propagate with a constant velocity or constant shape but can be affected by buoyancy-driven convection and/or intrinsic

thermal instabilities. Some of these phenomena significantly affect FP and must be considered; others are of more interest to those collecting nonlinear phenomena.<sup>80</sup>

#### 4.38.5.4 Starting Fronts

Fronts can be started by any process that will raise the starting materials to a temperature high enough that the rate of heat production will exceed heat loss. Three methods have been used. The most common is to use a thermoelectric heater such as a soldering iron. With benzoyl peroxide as the initiator, *N,N*-dimethylaniline can be added to cause the peroxide to rapidly decompose in the location in which it is added. The other method is to use a UV light with a system that contains both photoinitiator and thermal initiator. Ritter *et al.*<sup>81</sup> analytically considered the necessary conditions for ignition. Heifetz *et al.*<sup>82</sup> performed numerical simulations determining how the temperature of a constant temperature heat source affected the ability to initiate a front with heat loss.

Nason *et al.*<sup>83</sup> examined the conditions for photoinitiation of FP of trimethylolpropane triacrylate with Luperox 231 as the thermal initiator and Darocur 4265 as the photoinitiator. They found that there was an optimal concentration of photoinitiator to achieve the shortest start time for the front (Figure 6).

#### 4.38.5.5 Free-Radical Frontal Polymerization

Free-radical chemistry is the most amenable to FP because the reactions can be rapid, very exothermic, and with a high energy of activation controlled by the type of initiator. A number of radical polymerization reactions are highly exothermic and able to support the FP regime. A free-radical polymerization with a thermal initiator can be approximately represented by a

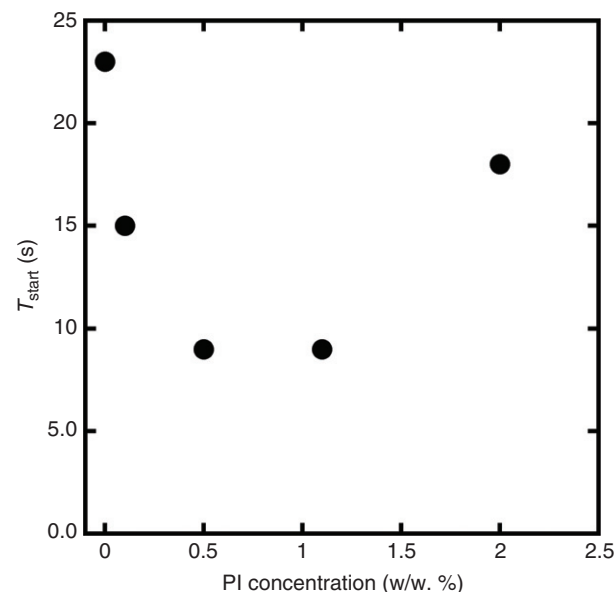


**Figure 6** The time until front ignition as a function of photoinitiator concentration for irradiance of  $5.9 \text{ mW cm}^{-2}$  with 0.4 wt.% Luperox 231 for trimethylolpropane triacrylate. Adapted from Nason, C.; Roper, T.; Hoyle, C.; Pojman, J. A. *Macromolecules* **2005**, *38*, 5506–5512.<sup>83</sup>

three-step mechanism. First, an unstable compound, usually a peroxide or nitrile, decomposes to produce radicals:



where  $f$  is the efficiency, which depends on the initiator type and the solvent. A radical can then add to a monomer to initiate a growing polymer chain:



The propagation step [3] continues until a chain terminates by reacting with another chain (or with an initiator radical):



The major heat release in the polymerization reaction occurs in the propagation step. However, the propagation step does not have a sufficiently high activation energy to permit a front. FP autocatalysis is controlled by the energy of activation of the initiator decomposition. The steady-state assumption in the polymerization model gives an approximate relationship between the effective activation energy of the entire polymerization process and activation energy of the initiator decomposition reaction:

$$E_{\text{eff}} = E_p + \left(\frac{E_i}{2}\right) - \left(\frac{E_t}{2}\right) \quad [5]$$

where  $E_p$  is the activation energy of the propagation step,  $E_i$  is that for the initiator decomposition, and  $E_t$  is that for the termination step.

The second term in the right-hand side of eqn [5] depends on the initiator. Because it has the largest magnitude, this value mostly determines the effective activation energy. Because of this, the initiator plays a significant role in determining if a front will exist, and if so, temperature profile in the front and how fast the front will propagate.

#### 4.38.5.6 Properties of Monomers

Some requirements on the physical properties of the polymerization medium itself must also be met. In the early papers on FP, the authors<sup>49–52</sup> applied very high pressure (up to 5000 atm) to eliminate monomer boiling (methyl methacrylate) and the reaction zone decay due to the density gradient in the reaction zone (Rayleigh-Taylor instability). They also managed to observe only downward traveling fronts because natural convection rapidly removed heat from the reaction zone of an ascending front leading to extinction. However, at pressures less than 1500 atm, descending fronts decayed because the polymer was denser than the monomer. Thus, unless a sufficiently high pressure is applied, it is not possible to obtain a polymerization front with methyl methacrylate (Figure 7).

We describe cases when FP is expected to be observed. The first case is the polymerization of crosslinking monomers (thermosets). The second group of monomers form polymers that are insoluble in the monomer. Good examples are acrylic and methacrylic acids.<sup>54,84,85</sup> Insoluble polymer particles adhere to each other during their formation and stick to the reactor or test tube walls, forming a mechanically stable phase and discernible polymer–monomer interface. Nonetheless, Rayleigh–Taylor and double-diffusive instabilities, which we will discuss

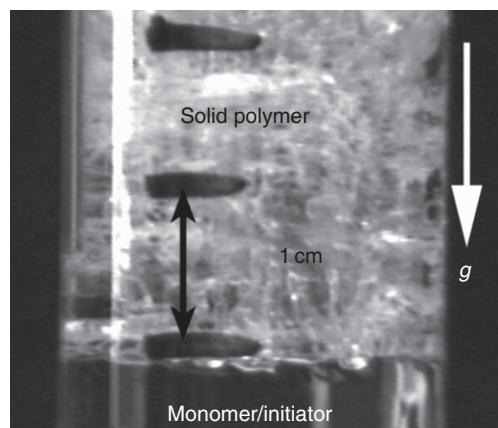


**Figure 7** A descending front of triethylene glycol dimethacrylate polymerization with benzoyl peroxide as the initiator.

in Section 4.38.5.16.1, partially develop in such systems and manifest themselves as fingering.<sup>54,86</sup> How well the front sustains itself depends on conversion, the polymer glass transition temperature, and molecular weight distribution. Indeed, these properties themselves depend on the initial reactant temperature, initiator type, and concentration.<sup>84</sup>

Nagy and Pojman developed a technique to suppress fingering with methacrylic acid fronts in which the tube was rotated around the axis of front propagation.<sup>87</sup> The front velocity depended on the fourth power of the rotational frequency, and the amplitude of the front curvature was proportional to the square of the frequency.

The third group of monomers includes all highly reactive monomers that produce thermoplastic polymers, which are molten at the front temperature. Such fronts decay due to the Rayleigh–Taylor instability. Although these polymers are soluble in their monomers (given sufficient time), on the time scale of the front the polymer is effectively immiscible with the monomer. Adding inert filler such as ultrafine silica gel or a soluble polymer increases the viscosity and eliminates the front collapse. Some monomers such as styrene and methyl methacrylate require moderate pressure (20–30 atm) to eliminate monomer boiling. Higher-boiling-temperature monomers like butyl acrylate support the frontal regime at ambient pressure in test tubes. FP of the third group of monomers can be realized in any orientation because the large viscosity (of the monomer–Cabosil system) suppresses natural convection.

All FP monomers should be highly reactive to maintain the reaction in the presence of heat losses that always occur, and are especially important in narrow tubes. The frequency factor for the propagation rate coefficient should be at least  $A_p \geq 10^5 \text{ l mol}^{-1} \text{ s}^{-1}$ , based on experience with reactions in the test tubes with less than 3 cm diameter at ambient temperature. A polymerization front is a thermal wave having existence conditions with respect to the heat loss intensity. In some cases, the problem of quenching can be solved by using larger diameter test tubes or preheating the initial reactants. Preheating will not work with a fast decomposing initiator, for example, AIBN, because of the homogeneous reaction in the bulk monomer.

#### 4.38.5.7 Frontal Polymerization in Solution

FP of several reactive monomers can be performed in high boiling point solvents.<sup>88</sup> Acrylamide polymerization will propagate in water (with some vaporization of water),<sup>89,90</sup> in dimethyl sulfoxide (DMSO)<sup>91</sup> and in dimethyl formamide (DMF) with several initiators, including sodium persulfate, potassium persulfate, ammonium persulfate, and benzoyl peroxide. Interestingly, no gas bubbles are observed with acrylamide/persulfate in DMSO. (The persulfates do not produce volatile side products.) Several other monomers also work in these solvents, including acrylic acid, sodium methacrylate, and zinc dimethacrylate.<sup>88</sup>

For a monomer to support FP in a solvent, the enthalpy of the reaction must be sufficiently high that dilution does not lower the front temperature below a front-sustaining value. Dimethylbenzene can be used with polyurethane synthesis.<sup>92</sup>

Fronts of acrylamide in DMSO (1:1) are not destroyed by the Rayleigh–Taylor instability (‘fingering’) because the polyacrylamide gels. However, a monomer such as acrylic acid, which does not gel in DMSO, exhibits rampant fingering and will not propagate without the addition of a few percent of bisacrylamide (a difunctional monomer), which produces a crosslinked and solid product. The same is true for acrylamide in DMF.

#### 4.38.5.8 Temperature Profiles

A polymerization front has a very sharp temperature profile, and profile measurements can provide much useful information. The temperature profiles help elucidate the reasons for incomplete conversion and the structure of the front. Two temperature profiles measured during FP of methacrylic acid are shown in Figure 8. The first profile is for benzoyl peroxide in methacrylic acid at different initial temperatures. The other profile was obtained for the same monomer with *tert*-butyl peroxide (*t*BPO). Conversion is directly proportional to the

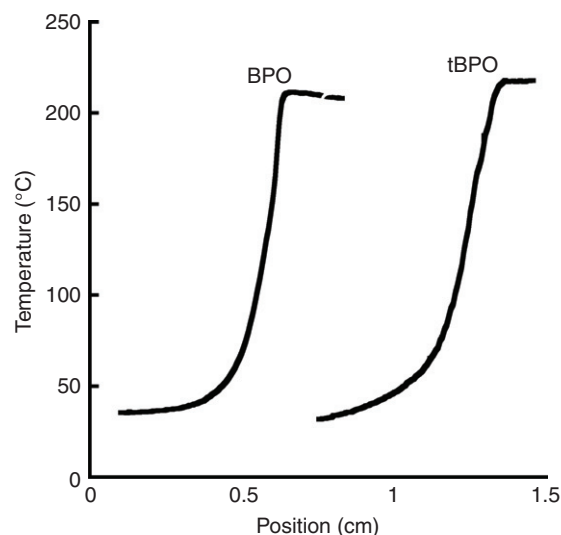


**Figure 8** Spatial temperature profiles for methacrylic acid polymerization fronts: 2% w/v of benzoyl peroxide (BPO), 12.5% v/v of *tert*-butyl peroxide (*t*BPO). Adapted from Pojman, J. A.; Ilyashenko, V. M.; Khan, A. M. *J. Chem. Soc. Faraday Trans.* **1996**, *92*, 2825–2837.<sup>55</sup>

difference between the maximum and initial temperatures. The *t*BPO profile reflects the use of a more stable initiator, which led to the highest conversion and widest heat conductivity zone. All these facts point to initiator burn out, that is, when the initiator has been exhausted before the reaction has been completed, more stable initiators give higher conversion. The methacrylic acid front with *t*BPO was significantly slower in spite of having the highest reaction temperature. This means that the effective activation energy of a polymerization front is directly correlated to the activation energy of the initiator decomposition, as was expected.

#### 4.38.5.9 Velocity Dependence on Initiator Concentration

Chechilo *et al.*<sup>52</sup> studied methyl methacrylate polymerization with benzoyl peroxide as the initiator. By placing several thermocouples, they could infer the front velocity and found a 0.36 power dependence for the velocity on the benzoyl peroxide concentration. More detailed studies for several initiators showed 0.223 for *t*BPO, 0.324 for BPO, and 0.339 for cyclohexylperoxide carbonate.<sup>50</sup>

Pojman *et al.* reported a detailed study of Triethylene glycol dimethacrylate (TGDMA) FP.<sup>84</sup> The power functional dependence for velocity versus initiator concentration was different for all three: AIBN (0.20), BPO (0.23), and LPO (0.31).

Khanukaev *et al.*<sup>93,94</sup> considered the theory of front propagation in terms of conversion and velocity as a function of initial temperature. Because of the high front temperature, all the initiator can decompose before all the monomer has reacted. The result is initiator 'burn out', which decreases conversion and velocity. High initial temperatures exacerbate this effect. Using their theory, they correctly predicted the conversion for one experiment with methyl methacrylate (46%) and a velocity of 0.12 cm min<sup>-1</sup>.

The most careful study of velocity as a function of experimental parameters was performed by Goldfeder *et al.*<sup>95</sup> They considered the FP of butyl acrylate containing fumed silica (to suppress convection) in a custom-built reactor that allowed temperature control at 50 atm pressure (to suppress bubbles). They developed analytical solutions for the front velocity as a function of initiator concentration and initial temperature.

#### 4.38.5.10 Front Velocity as a Function of Temperature

The front velocity is a function of the initial temperature and the  $\Delta T$  of the reaction, where  $\Delta T$  is determined by the  $|DH| \times M_0/C_p$ . The value of  $\Delta T$  is also affected by the presence of any inert material. Goldfeder *et al.*<sup>95</sup> derived an expression for the front velocity in terms of the parameters for a free-radical polymerization. The velocity is a function of  $\kappa$ , the thermal diffusivity (0.0014 cm<sup>2</sup> s<sup>-1</sup>),  $T_b$ ,  $k_d^0$  = the preexponential factor for the initiator decomposition ( $4 \times 10^{12}$  s<sup>-1</sup>),  $E_1 = E_d$  = the energy activation for the dissociation constant for the initiator = 27 kcal mol<sup>-1</sup>,  $R_g$  is the ideal gas constant.

$$u^2 = \frac{\kappa R_g T_b^2}{2E_1(T_b - T_0)} k_d^0 e^{-E_d/R_g T_b} \quad [6]$$

The model worked well for butyl acrylate. Figure 9 shows the results for the experiment and analytical solution as well as

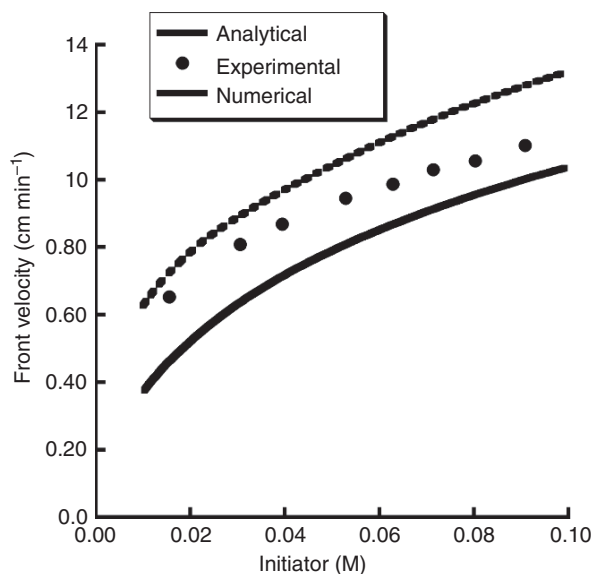


**Figure 9** Comparison of the velocity dependence on the AIBN concentration for the frontal polymerization of butyl acrylate at 278 K, determined experimentally, numerically and analytically. Adapted from Goldfeder, P. M.; Volpert, V. A.; Ilyashenko, V. M.; *et al. J. Phys. Chem. B* **1997**, *101*, 3474–3482.<sup>95</sup>

numerical simulations with the complete model. This model does not work with multifunctional monomers.

#### 4.38.5.11 The Effect of Type of Monomer and Functionality on Front Velocity

Fronts with methacrylates propagate more slowly than with acrylates, as would be expected from the lower reactivity of the methacrylate. Nason *et al.*<sup>83</sup> studied the velocity for many different acrylates and methacrylates (Figure 10). In Figure 11, we can see how the front velocity varies with the inverse of the molecular weight per acrylate group. Front velocities can reach as high as 50 cm min<sup>-1</sup> for both triacrylates and tetraacrylates with high concentrations of initiator.

The high velocity is consistent with the behavior of multifunctional acrylates. Once gelation occurs, the rate of termination decreases and so the overall rate of polymerization increases. Thus, the multifunctional acrylates exhibit an extreme gel effect that causes them to polymerize very rapidly. This crosslinking also affects the manner of front propagation, as we will discuss in section 4.38.5.16.4.

#### 4.38.5.12 Solid Monomers

Pojman *et al.*<sup>96</sup> demonstrated that acrylamide could be polymerized frontally without solvent. Using a rock tumbler, they ground acrylamide and various solid initiators, including benzoyl peroxide, AIBN, potassium persulfate, ceric ammonium nitrate, ceric ammonium sulfate, bromate/malonic acid, lead dioxide, and lithium nitrate. The conversion was determined by adding bromine<sup>97</sup> and titrating the excess iodometrically.<sup>98</sup> The number of growing chains that are terminated by an initiator radical (primary termination) increases with higher concentrations of initiator, decreasing conversion. The degree

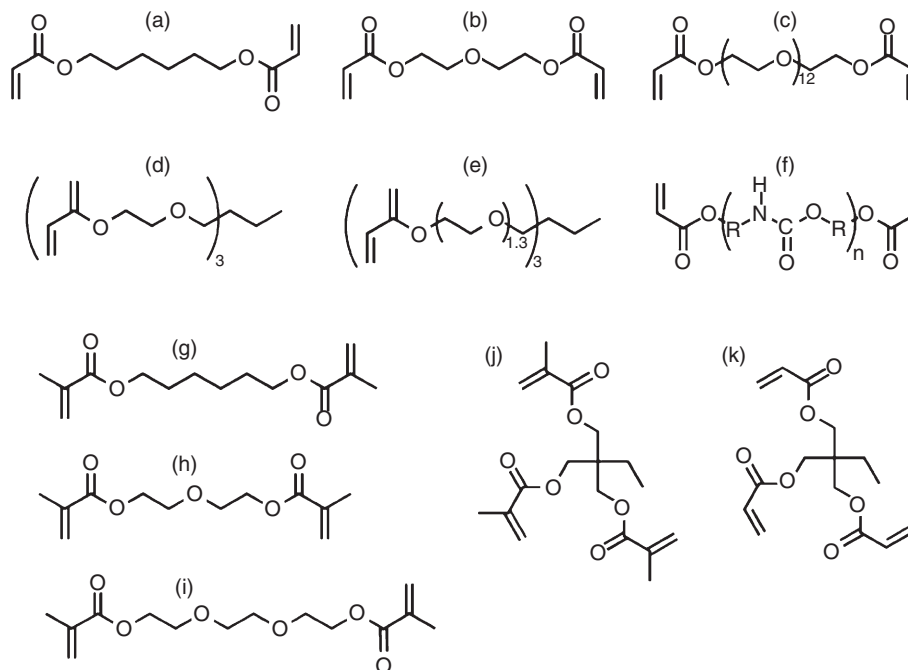


**Figure 10** Chemical structures of some acrylate and methacrylate monomers: (a) hexanediol diacrylate (HDDA), (b) diethylene glycol diacrylate (DEGDA), (c) poly(ethylene glycol) diacrylate (PEGDA), (d) trimethylolpropane ethoxy triacrylate (TMPEOTA-I), (e) trimethylolpropane ethoxy triacrylate (TMPEOTA-II), (f) difunctional urethane acrylate (Ebecryl 8402), (g) hexanediol dimethacrylate (HDDMA), (h) diethylene glycol dimethacrylate (DEGDMA), (i) triethylene glycol dimethacrylate (TREGDMA), (j) trimethylolpropane trimethacrylate (TMPTMA), (k) trimethylolpropane triacrylate (TMPTA). Reprinted with permission from Nason, C.; Roper, T.; Hoyle, C.; Pojman, J. A. *Macromolecules* **2005**, *38*, 5506–5512.<sup>83</sup> Copyright 2005 American Chemical Society.

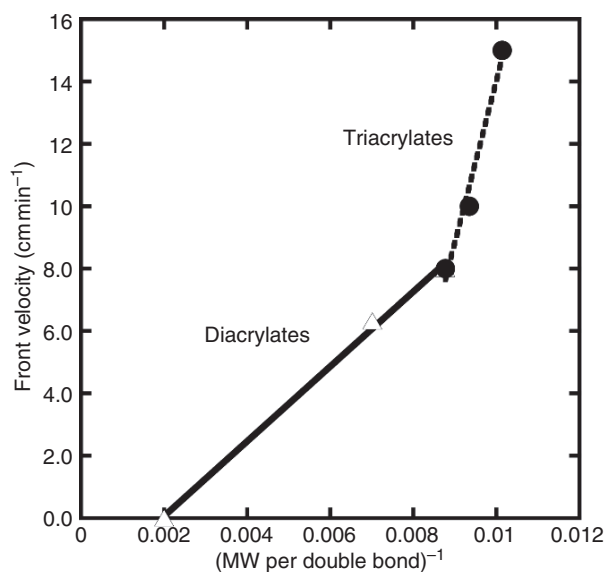


**Figure 11** Velocity versus MW per double bond; 1 wt.% Luperox 231, 2 wt.% Darocur 4265; In air: Monomers and MW per double bond; PETA-K, 91; TMPTA, 99; DPHA, 105; DEGDA, 107; HDDA, 113; DPGDA, 121; TMPEOTA, 143; TMPEOTA, 201; PEGDA, 350; Ebecryl 8402, 500; irradiance of 5.9 mW cm<sup>-2</sup>. Adapted from Nason, C.; Roper, T.; Hoyle, C.; Pojman, J. A. *Macromolecules* **2005**, *38*, 5506–5512.<sup>83</sup>

of monomer conversion with AIBN was strongly dependent on the initiator concentration, with 0.8% AIBN, 95% of the monomer reacted but only 50% reacted with 2% AIBN.

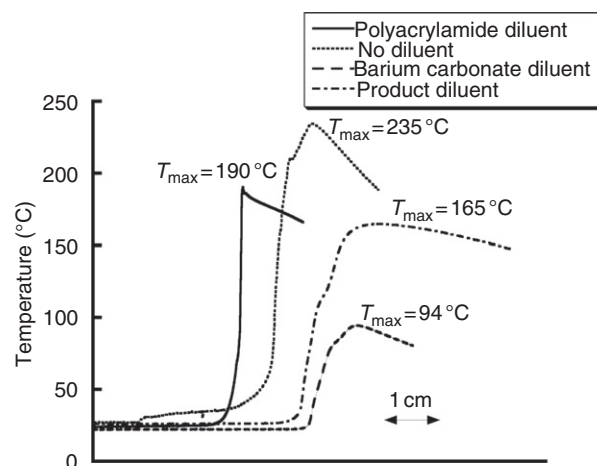


**Figure 12** Temperature profiles for the frontal polymerization of undiluted acrylamide, of acrylamide diluted with commercial polyacrylamide, of acrylamide diluted with barium carbonate, and of acrylamide diluted with frontally polymerized acrylamide. Adapted from Fortenberry, D. I.; Pojman, J. A. *J. Polym. Sci. Part A: Polym. Chem.* **2000**, *38*, 1129–1135.<sup>99</sup>

The front velocities were about on the order of 10 cm min<sup>-1</sup>. The higher velocities compared to monoacrylates resulted from high front temperatures (272 °C compared to 190 °C) and the greater reactivity of acrylamide.

Fortenberry and Pojman<sup>99</sup> studied FP of acrylamide in detail. Synthesis of polyacrylamide via FP resulted in a cross-linked, insoluble product. Figure 12 shows that the maximum

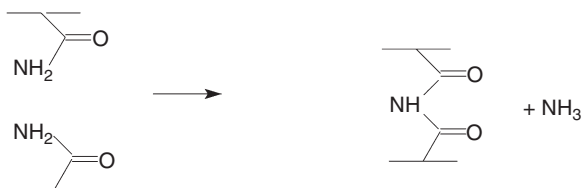


**Figure 13** The scheme for intermolecular imidization, as occur in the frontal polymerization of acrylamide.

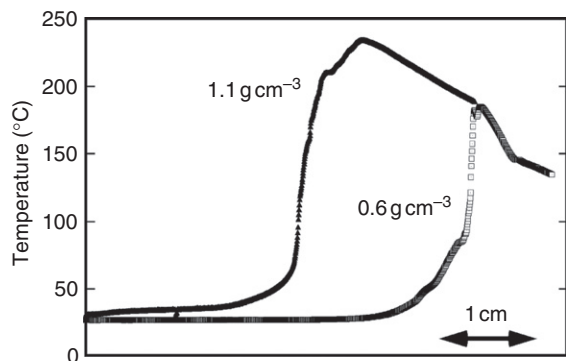


**Figure 14** Temperature profiles of the frontal polymerization of acrylamide with potassium persulfate as the initiator, at two different initial densities. Adapted from Fortenberry, D. I.; Pojman, J. A. *J. Polym. Sci. Part A: Polym. Chem.* **2000**, *38*, 1129–1135.<sup>99</sup>

front temperature reached during polymerization was 235 °C. The presence of ammonia was detected by scent and litmus paper, which indicated imidization occurred (Figure 13). Analogous crosslinking by anhydride formation was observed in the FP of methacrylic acid (see section 4.38.5.14).<sup>100</sup> They calculated that the frontally produced samples were only 6% imidized. Imidization was prevented by adding an inert filler, either barium carbonate or polyacrylamide. Fronts propagated with front temperatures as low as 97 °C (Figure 14).

Foretenberry and Pojman<sup>99</sup> found that the front velocity was not a function of the particle size of the ground acrylamide but was a function of the green (unreacted) density. The velocity increased with the increased green density because the front temperature was higher and the thermal diffusivity larger. Fronts can even propagate if the sample is immersed in liquid nitrogen, provided a change of temperature of 400 K (Figure 15).

Pomogailo and his co-workers studied interesting solid systems that require no added initiator but proceed by a free-radical mechanism.<sup>101–109</sup> Using transition-metal complexes with acrylamide, they achieved FP with the solid monomers.

#### 4.38.5.13 Effect of Pressure

Pojman *et al.*<sup>55</sup> performed experiments in a custom-built reactor that allowed isobaric and isothermal conditions. They found that the front velocity was a function of the applied pressure, even at low values of less than 30 atm. As the pressure is increased, the velocities decrease, exactly opposite the behavior observed by Chechilio and Enikolopyan at high pressures!

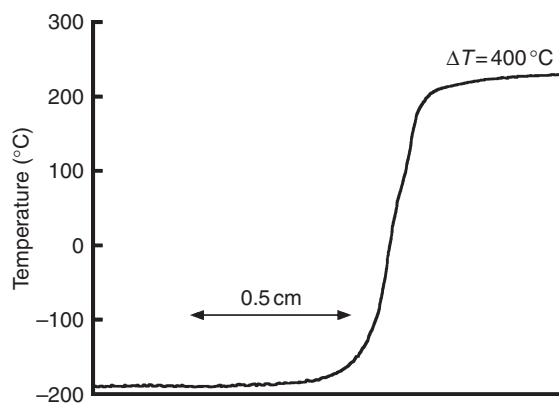


**Figure 15** The temperature profile of frontal polymerization of acrylamide immersed in liquid nitrogen. Adapted from Pojman, J. A.; Ilyashenko, V. M.; Khan, A. M. *J. Chem. Soc. Faraday Trans.* **1996**, *92*, 2825–2837.<sup>55</sup>

At the low pressures we employ, we are not affecting the rate constants of polymerization but suppressing bubbles.

There are three sources of bubbles. All thermal initiators (except for persulfates), produce volatile byproducts, such as CO<sub>2</sub>, methane, or acetone. It is an inherent problem with all commercially available peroxide or nitrile initiators.

Another source of bubbles is dissolved gas and water in the monomer. Gases can be removed under vacuum but water is extremely difficult to remove from methacrylic acid and TGDMA. Less than 1 mg of water will result in 2 cm<sup>3</sup> of water vapor at the front temperature of 200 °C and 1 atm of pressure. The only certain solution to all three sources is to perform reactions under pressure.

Bubbles can increase the velocity of fronts in standard closed test tubes initially at ambient pressure by as much as 30% compared to fronts free of bubbles under high pressure. The expansion of bubbles is part of the velocity by forcing unreacted monomer up and around the cooling polymer plug that is contracting; poly(methacrylic acid) is about 25% more dense than its monomer. This means that the pressure increases during the reaction because the tube is sealed, except for leakage around the initial polymer plug.<sup>86</sup>

Figure 16 shows the front velocity as a function of the inverse of the applied pressure. As the pressure was increased the velocity decreased because the volume of the bubbles was decreased, following Boyle's law.

We can write the velocity as

$$\text{vel}(p) = \text{vel}_0 + \frac{\text{Const}}{p} \quad [7]$$

where the constant is a function of the number of moles of gas produced in the front. Therefore, the higher the initiator concentration, the higher is the applied pressure necessary to obtain the true front velocity.

To determine the true front velocity dependence on initiator concentration requires that the effect of bubbles be eliminated. Different initiators can yield different amounts of gas. Thus, the velocity depends not only on the kinetics of the initiator decomposition, but also on the amount of gas produced and on the applied pressure.

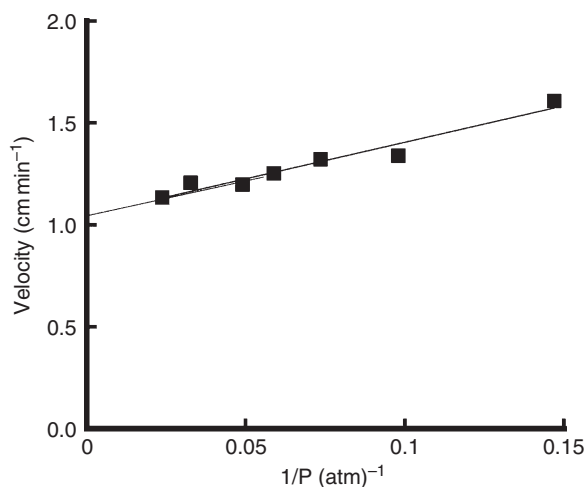


**Figure 16** Front velocity of butyl acrylate polymerization as a function of applied pressure with AIBN as the initiator (1.7% w/w) and 5.7% fumed silica. Adapted from Pojman, J. A.; Ilyashenko, V. M.; Khan, A. M. *J. Chem. Soc. Faraday Trans.* **1996**, *92*, 2825–2837.<sup>55</sup>

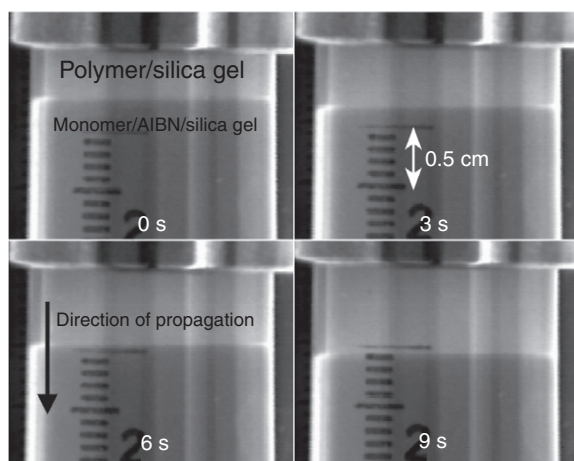


**Figure 17** A front of butyl acrylate polymerization with fumed silica (to prevent convection) and with 4% AIBN, under 50 atm pressure. Adapted from Pojman, J. A.; Ilyashenko, V. M.; Khan, A. M. *J. Chem. Soc. Faraday Trans.* **1996**, *92*, 2825–2837.<sup>55</sup>

Poly(methacrylic acid) formed in a front in a test tube initially at ambient pressure is opaque but translucent when produced under at least 34 atm pressure. Very small bubbles scatter light and make the material opaque when in fact, the polymer itself is clear. This is also true with butyl acrylate fronts. Cabosil has a refractive index close enough to poly(butyl acrylate) that the initial solution and product are translucent, as can be seen in Figure 17.

If TGDMA was partially reacted to produce a gel before front initiation, no bubbles appear as the front propagates. (Gelling was accomplished by allowing TGDMA/initiator to sit at room temperature for several days or by heating to 40 °C until gelation occurs.) In ungelled TGDMA, copious bubble production occurs. It seems that the gel prevents nucleation of bubbles before complete crosslinking makes it impossible to form bubbles.

To reduce bubble formation, there are several approaches besides using applied pressure. Some peroxides produce less

gas. Let us consider more about why peroxide and nitriles produce volatile compounds. The decomposition of a peroxide is endothermic and reversible. To make the production of radicals irreversible, initiators fragment (Figure 18). For example, AIBN decomposes to produce N<sub>2</sub> and organic radicals, making the overall reaction exothermic and irreversible. Benzoyl peroxide decomposes into the benzoyl radical, which fragments into carbon dioxide and a phenyl radical. Dicumyl peroxide breaks into peroxy radicals that undergo beta scission to produce acetophenone and methyl radicals. 1,1-Di(*tert*-butylperoxy)-3,3,5-trimethylcyclohexane (Luperox 231) is a room-temperature stable liquid that readily dissolves in acrylates. Upon decomposition and beta scission, it produces acetone and methyl radicals and a diperoxy radical.

Persulfate does not produce bubbles. Pojman *et al.*<sup>88</sup> used ammonium persulfate in the solution polymerization of acrylamide in DMSO. Persulfate salts are not soluble in organics; so Masere *et al.*<sup>40</sup> synthesized trioctylmethyl ammonium persulfate, which is a room temperature ionic liquid. Mariani *et al.*<sup>110</sup> synthesized phosphonium-based persulfate ionic liquids, which had less of a plasticization effect because of their lower molecular weight.

#### 4.38.5.14 Molecular Weight Distribution

Pojman *et al.*<sup>100</sup> examined the molecular distribution of two systems: methacrylic acid and butyl acrylate. Previously Pojman *et al.*<sup>86</sup> had determined the molecular weight of poly(methacrylic acid) produced frontally and reported very high molecular weight (about 10<sup>6</sup> g mol<sup>-1</sup>), which did depend on the radial position in the sample. Methacrylic acid can undergo anhydride formation, leading to branched polymers of higher molecular weight than expected. Using morpholine to selectively cleave the anhydride linkages, they determined that the degree of polymerization was about 100 and that about 20% of the carboxyl groups were in the anhydride form. After cleavage, the molecular weight was in the expected range (Figure 19). Poly(butyl acrylate) prepared frontally produced the expected molecular weight ranges (Figure 20).

Fortenberry and Pojman<sup>99</sup> determined by light scattering that polyacrylamide prepared frontally with barium carbonate as an inert diluent had a molecular weight average on the order of 10<sup>6</sup>.

Enikolopyan *et al.*<sup>111</sup> analytically considered the problem of the molecular weight distribution when the consumption of initiator was included. Not surprisingly, the distributions were more broad than observed in an isothermal polymerization, but no supporting experimental data were presented.

In order to produce the poly(butyl acrylate), silica gel was added to increase the viscosity and avoid convective mixing.<sup>100</sup> (We will discuss convective instabilities in section 4.38.5.16.1). Because high viscosity leads to high molecular weight via the gel effect, Pojman *et al.*<sup>112</sup> sought to prepare poly(butyl acrylate) frontally but without added silica. In order to accomplish this, they flew an experiment on a sounding rocket in order to avoid buoyancy-driven convection. They found that the molecular weight distribution was the same as that prepared in the lab using silica gel. Thus, they concluded that the silica increased the macroscopic viscosity but did not affect the molecular-level viscosity.

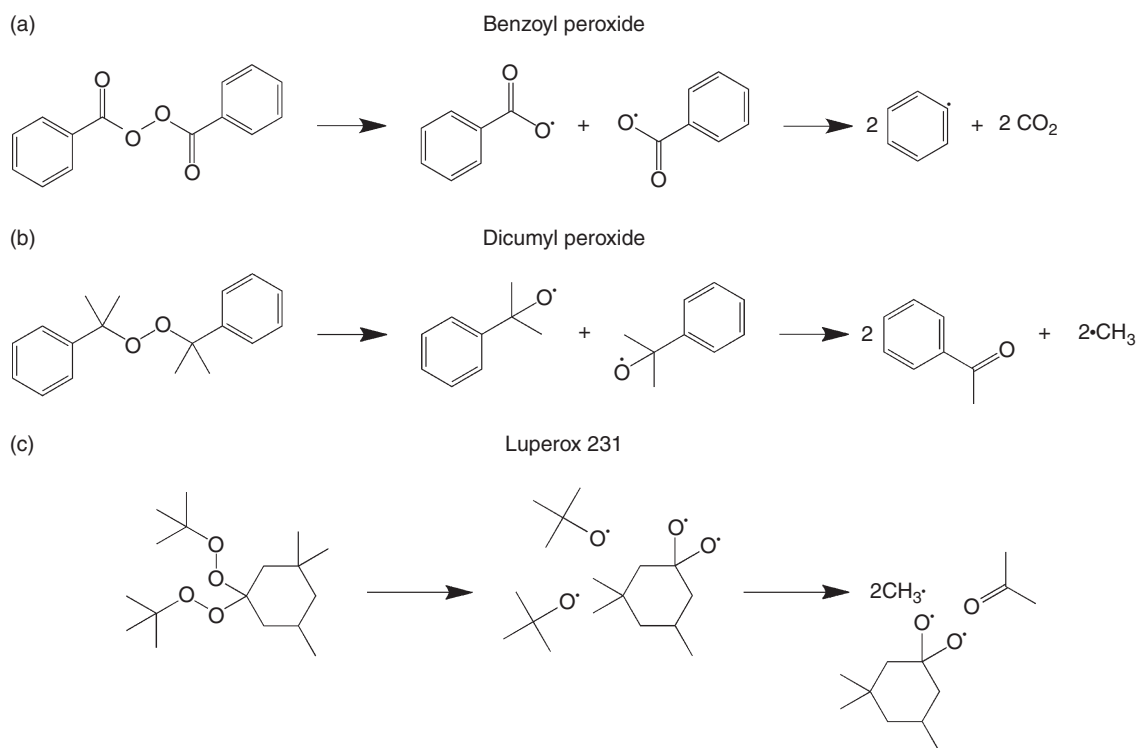


**Figure 18** The decomposition schemes for three different initiators.

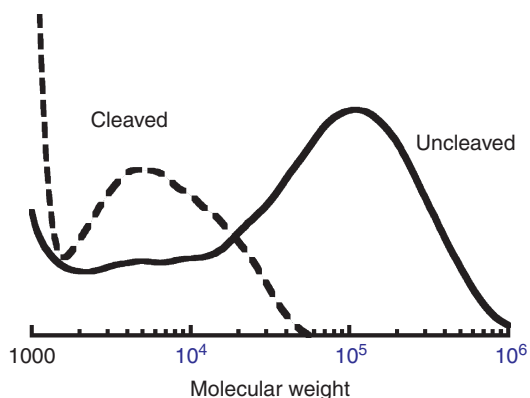


**Figure 19** The molecular weight distribution for frontally prepared poly(methacrylic acid) and after the anhydride linkages were cleaved with morpholine. Adapted from Pojman, J. A.; Willis, J. R.; Khan, A. M.; West, W. W. *J. Polym. Sci. Part A: Polym. Chem.* **1996**, *34*, 991–995.<sup>100</sup>

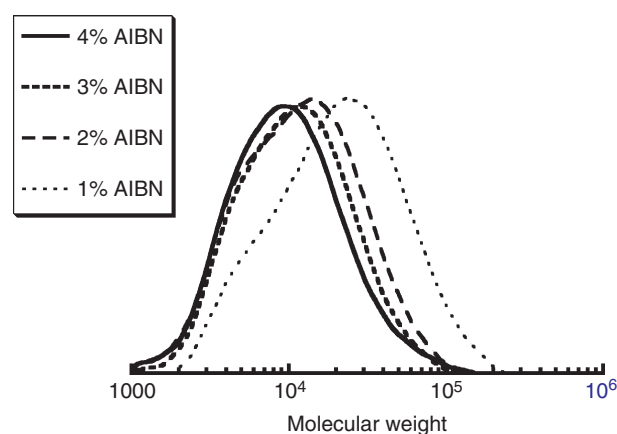


**Figure 20** The molecular weight distributions for poly(butyl acrylate) produced frontally. Adapted from Pojman, J. A.; Willis, J. R.; Khan, A. M.; West, W. W. *J. Polym. Sci. Part A: Polym. Chem.* **1996**, *34*, 991–995.<sup>100</sup>

#### 4.38.5.15 Conversion

An important issue for using FP for polymer synthesis is conversion. We will consider in Section 4.38.5.26 the advantages of FP, some of which will be rapid conversion without the use of solvent. However, if conversion is low and the product must be purified, those advantages will be nonexistent. Initiator 'burn out' occurs when the all the initiator has decomposed before the monomer has been completely reacted.<sup>93,94</sup> For methacrylic acid polymerization with benzoyl peroxide as the initiator, conversion ranged from 80% to below 70% in a 2.2-cm tube (Figures 21 and 22).<sup>84</sup> The conversion was higher in a 1.5-cm diameter tube (85–80%) because the front

temperature was lower due to greater heat loss in a narrower tube. With the more stable *t*BPO as the initiator in a 2.2-cm tube, conversion was significantly higher (92%) but the front velocity was lower, by as much as a factor of 2. Tredici *et al.*<sup>113</sup> found conversion around 90% for a copolymerization.

By combining the two peroxides, the conversion could be obtained as high as for *t*BPO alone with a velocity close to that with BPO alone. The front velocity was determined by the less stable peroxide, BPO, with the more stable *t*BPO finishing the reaction. However, the velocity was lower than for BPO alone, and the authors proposed that the radicals from the BPO decomposition could induce decomposition of the *t*BPO.

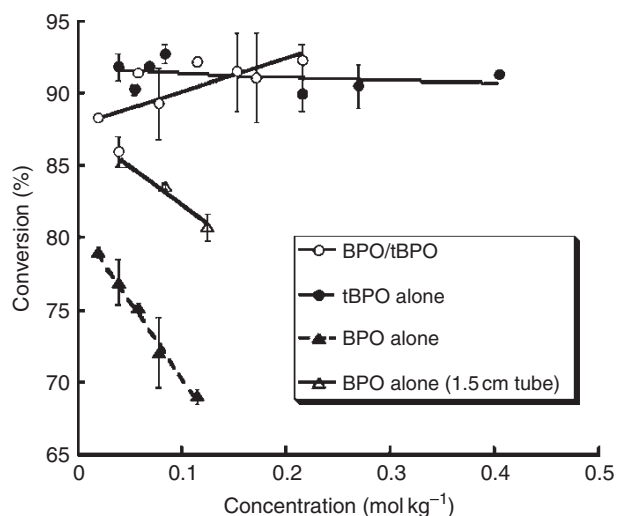


**Figure 21** The conversion of methacrylic acid frontal polymerization as a function of benzoyl peroxide (BPO) and/or *tert*-butyl peroxide (tBPO). Adapted from Pojman, J. A.; Willis, J.; Fortenberry, D.; *et al. J. Polym. Sci. Part A: Polym. Chem.* **1995**, *33*, 643–652.<sup>84</sup>

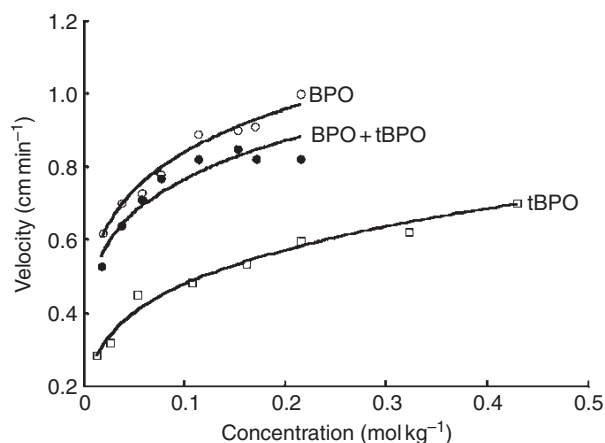


**Figure 22** The velocity for methacrylic acid frontal polymerization with benzoyl peroxide (BPO) and *tert*-butyl peroxide (tBPO). Adapted from Pojman, J. A.; Willis, J.; Fortenberry, D.; *et al. J. Polym. Sci. Part A: Polym. Chem.* **1995**, *33*, 643–652.<sup>84</sup>

Conversion can also be limited by thermodynamics. Because the polymerization reactions are exothermic, the equilibrium conversion decreases with increasing temperature.<sup>114</sup> A relationship between temperature and the equilibrium monomer concentration (assuming unit activity coefficients) can be derived,<sup>55</sup> in which  $[M]_0$  is the standard monomer concentration used to calculate the  $\Delta S^0$  and  $\Delta H^0$ .

$$T = \frac{\Delta H_0}{\Delta S^0 + R \ln([M]_{\text{eq}}/[M]^0)} \quad [8]$$

For an adiabatic polymerization, the maximum conversion is uniquely determined by the  $\Delta H^0$  and  $\Delta S^0$  of polymerization. As the temperature increases, the equilibrium conversion is reduced and can be related by

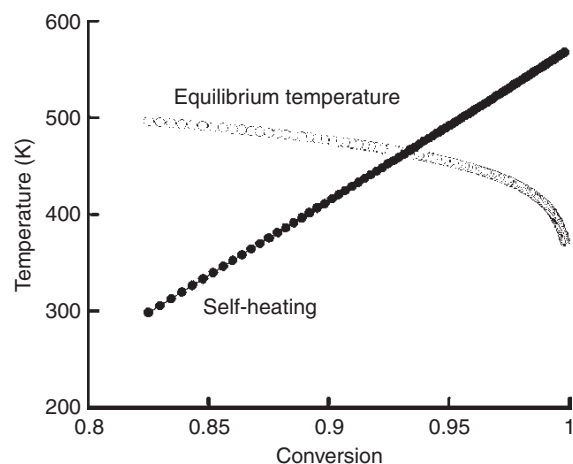


**Figure 23** The relationship between the extent of conversion and the ceiling temperature for methyl methacrylate.  $[M]_{\text{initial}} = 9.36 \text{ M}$ ,  $\Delta H^0 = -56 \text{ kJ mol}^{-1}$ ,  $\Delta S^0 = 117 \text{ J K}^{-1}$ ,  $C_p = 205.3 \text{ J mol}^{-1} \text{ K}^{-1}$ ,  $T_i = 25 \text{ }^\circ\text{C}$ . Adapted from Pojman, J. A.; Ilyashenko, V. M.; Khan, A. M. *J. Chem. Soc. Faraday Trans.* **1996**, *92*, 2825–2837.<sup>55</sup>

$$\alpha = 1 - \frac{1}{[M]_{\text{initial}}} \exp\left(\frac{\Delta H^0 - T\Delta S^0}{RT}\right) \quad [9]$$

The relationship for the temperature and conversion for adiabatic self-heating is

$$T = T_i + \frac{\alpha\Delta H^0}{C_p} \quad [10]$$

The solution of eqns [8] and [9] provides the conversion achieved in adiabatic polymerization. Figure 23 shows the results for methyl methacrylate with an initial temperature of 25 °C, using thermodynamic data from Odian.<sup>115</sup> The conversion is 0.93, which means that independent of initiator burnout, complete conversion can never be achieved because of the high front temperature. This value is very sensitive to the exact values of the thermodynamic parameters so the calculated value may not correspond precisely to experiment. Nonetheless, thermodynamics must be considered when selecting candidates for FP. Similar monomers may exhibit very different conversions at the same temperature. For example, zero conversion will be obtained at 310 °C with styrene but  $\alpha$ -methylstyrene will not react above 61 °C.<sup>115</sup>

#### 4.38.5.16 Interferences with Frontal Polymerization

##### 4.38.5.16.1 Buoyancy-driven convection

Because of the large thermal and concentration gradients, polymerization fronts are highly susceptible to buoyancy-induced convection. Garbey *et al.*<sup>116–118</sup> performed the linear stability analysis for the liquid–liquid and liquid–solid cases. The bifurcation parameter was a ‘frontal Rayleigh number’

$$R = \frac{g\beta q\kappa^2}{\nu c^3} \quad [11]$$

where  $g$  is the gravitational acceleration,  $\beta$  the thermal expansion coefficient,  $q$  the temperature increase at the front,  $\kappa$  the thermal diffusivity,  $\nu$  the kinematic viscosity, and  $c$  the front velocity.

Let us first consider the liquid–solid case. Neglecting heat loss, the descending front is always stable because it



**Figure 24** Left: The front on the left is descending and the one on the right ascending with an axisymmetric mode of convection. Right: An antisymmetric mode of an ascending front. The system is the acrylamide/bis-acrylamide polymerization in DMSO with persulfate initiator. Adapted from Bowden, G.; Garbey, M.; Ilyashenko, V. M.; *et al. J. Phys. Chem. B* **1997**, *101*, 678–686.<sup>119</sup>

corresponds to heating a fluid from above. The front is always flat. If the front is ascending, convection may occur depending on the parameters of the system. Bowden *et al.*<sup>119</sup> experimentally confirmed that the first mode is an antisymmetric one, followed by an axisymmetric one. **Figure 24** shows a flat descending front as well as axisymmetric and antisymmetric modes of ascending fronts. **Figure 25** shows the stability diagram in the viscosity-front velocity plane. Most importantly, they confirmed that the stability of the fluid was a function not only of the viscosity but also of the front velocity. This means that the front dynamics affects the fluids dynamics. McCaughey *et al.*<sup>120</sup> tested the analysis of Garbey *et al.* and found the same bifurcation sequence of antisymmetric to axisymmetric convection in ascending fronts as seen with the liquid–solid case.

If the reactor is not vertical, there is no longer a question of stability – there is always convection. Bazile *et al.*<sup>121</sup> studied descending fronts of acrylamide/bis-acrylamide polymerization in DMSO as a function of tube orientation. The fronts remained nearly perpendicular to the vertical but the velocity

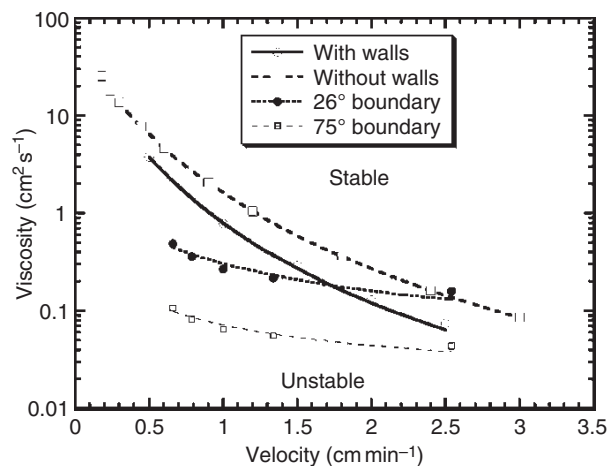


**Figure 25** The stability diagram for the system in **Figure 24**. Adapted from Bowden, G.; Garbey, M.; Ilyashenko, V. M.; *et al. J. Phys. Chem. B* **1997**, *101*, 678–686.<sup>119</sup>

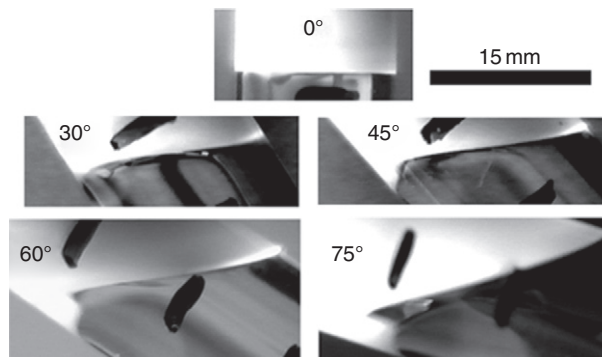


**Figure 26** The dependence of the front shape for descending fronts of acrylamide polymerization in DMSO with persulfate initiator. Adapted from Bazile, M., Jr.; Nichols, H. A.; Pojman, J. A.; Volpert, V. *J. Polym. Sci. Part A: Polym. Chem.* **2002**, *40*, 3504–3508.<sup>121</sup>

projected along the axis of the tube increased with  $1/\cos$  of the angle (**Figure 26**).

Liquid–liquid systems are more complicated than the previous case because a descending front can exhibit the Rayleigh–Taylor instability. The product is hotter than the reactant but is more dense (**Figure 27**), and because the product is a liquid, fingering can occur. Bidali *et al.*<sup>122</sup> described the phenomenon as the ‘rainstorm effect’. Such front degeneration is shown in **Figure 28**. The Rayleigh–Taylor instability can be prevented using high pressure,<sup>52</sup> adding a filler,<sup>95</sup> using a dispersion in salt water,<sup>123</sup> or performing the fronts in weightlessness.<sup>123</sup>

Texier-Picard *et al.*<sup>124</sup> analyzed a polymerization front in which the molten polymer was immiscible with the monomer and predicted that a front could exhibit the Marangoni instability even though the comparable unreactive fluids would not exhibit the instability. However, no liquid–liquid frontal system with an immiscible product has been identified. Even if such a system could be found, the experiment would have to be performed in weightlessness to prevent buoyancy-induced convection from interfering.

We note a significant difference between the liquid–liquid and the liquid–solid cases. For the liquid–solid case, convection in ascending fronts increases the front velocity but in the liquid–liquid case, convection slows the front. However, convection increases the velocity of pH fronts and Belousov-Zhabotinsky reaction waves.<sup>125,126</sup> Why is the difference between liquid–liquid FP and other frontal systems? In liquid–liquid systems, the convection also mixes cold monomer into the reaction zone, which lowers the front temperature. The front velocity depends more strongly on the front temperature than on the effective transport coefficient of the autocatalyst. Convection does not mix monomer into the reaction zone of a front with a solid product but rather increases thermal transport so the velocity is increased.

#### 4.38.5.16.2 Effect of surface tension-driven convection

If there is a free interface between fluids, gradients in concentration and/or temperature parallel to the interface cause gradients in the surface (interfacial) tension, which cause convection.<sup>127</sup> This convection, also known as Marangoni convection, is especially noticeable in thin layers (or weightlessness) in which buoyancy-driven convection is greatly reduced.

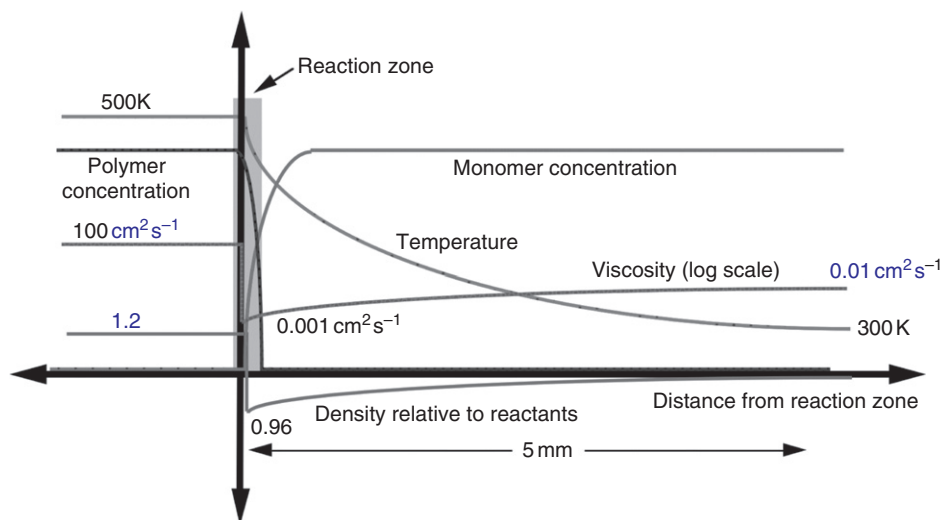


**Figure 27** Schematic diagram showing changes in properties across a propagating polymerization front that produces a thermoplastic. Courtesy of Paul Ronney.

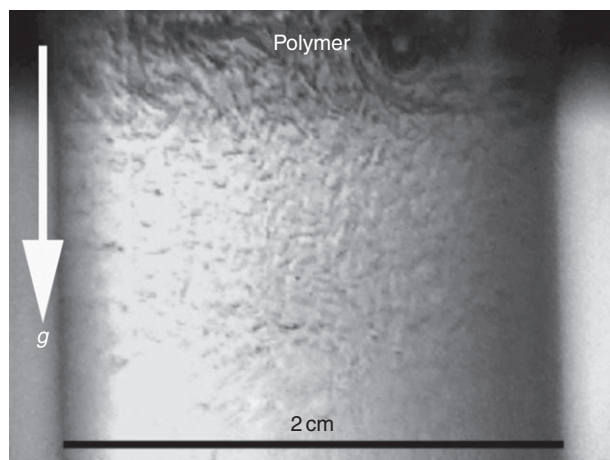


**Figure 28** Rayleigh–Taylor instability with a descending front of butyl acrylate polymerization.

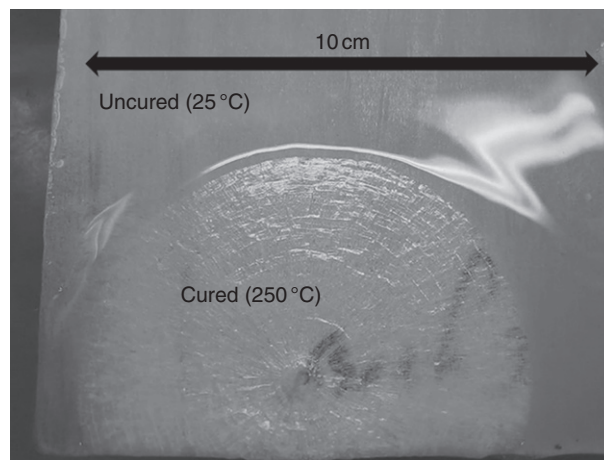


**Figure 29** A front of pentaerythritol tetraacrylate propagating in a thin layer on wood.

Asakura *et al.*<sup>128</sup> recently explained that FP was not applied to thin layers because it was thought that FP could not occur in thin layers. In fact, interfacial tension-driven convection can cause so much heat loss that fronts are quenched. **Figure 29** shows a front propagating in a thin layer (about 1 mm) of a tetraacrylate in which fumed silica is dispersed. The large temperature gradient created by the reaction ‘pushes’ monomer ahead but not enough to quench the front.

For a given surface, three variables affect whether a front will propagate, specifically, the viscosity (determined by the amount of fumed silica), the initiator concentration, and the thickness of the layer. For a fixed layer thickness, we determined that for trimethylolpropane triacrylate, with 2 phr silica, no front would propagate with 1 phr Luperox 231 but would propagate with 1.1 phr. (phr stands for ‘parts per hundred resin’.) **Figure 30** shows how complicated patterns can arise when the amount of silica was increased to 4 phr.

#### 4.38.5.16.3 Dispersion polymerization

Pojman *et al.* overcame the Rayleigh–Taylor instability by dispersing benzyl acrylate in a salt water solution whose density was greater than that of the polymer,<sup>123</sup> an approach that had been considered theoretically.<sup>129</sup> Fronts reached 200 °C, the same temperature as benzyl acrylate fronts with a diacrylate to prevent fingering. This indicated that the dispersion broke relatively quickly, leaving the monomer to polymerize in bulk and the salt water to settle to the lower section of the tube. The polymer was insoluble in tetrahydrofuran (THF) and in DMSO, and so they concluded that the acrylic acid formed then formed anhydride crosslinks.

#### 4.38.5.16.4 Thermal instabilities

Fronts do not have to propagate as planar fronts. Analogously to oscillating reactions, a front can exhibit periodic behavior, either as pulsations or as ‘spin modes’ in which a hot spot propagates around the reactor as the front propagates, leaving a helical pattern. This mode was first observed in SHS.<sup>130</sup> This



**Figure 30** A front propagating in a thin layer of a triacrylate with 4 phr fumed silica and 2.1 phr Luperox 231, a peroxide initiator.

general issue nonlinear behavior in FP has been considered in great detail.<sup>55,79,131,132</sup>

The linear stability analysis of the longitudinally propagating fronts in the cylindrical adiabatic reactors with one reaction predicted that the expected frontal mode for the given reactive medium and diameter of the reactor is governed by the Zeldovich number

$$Z = \frac{T_m - T_0}{T_m} \frac{E_{\text{eff}}}{RT_m} \quad [12]$$

For FP, lowering the initial temperature ( $T_0$ ), increasing the front temperature ( $T_m$ ), and increasing the energy of activation ( $E_{\text{eff}}$ ) all increase the Zeldovich number. The planar mode is stable if  $Z < Z_{\text{cr}} = 8.4$ . By varying the Zeldovich number beyond the stability threshold, subsequent bifurcations leading to higher spin mode instabilities can be observed. Second, for a cylindrical geometry, the number of spin heads or hot spots is also a function of the tube diameter. We point out that polymerization is not a one-step reaction, so that the above form of the Zeldovich number does not directly apply. However, estimates of the effective Zeldovich number can be obtained from the overall energy of activation with the steady-state assumption for free-radical polymerization.

The most commonly observed case with FP in tube is the spin mode in which a 'hot spot' propagates around the front. A helical pattern is often observed in the sample. The first case was with the FP of  $\epsilon$ -caprolactam,<sup>133,134</sup> and the next case was discovered by Pojman *et al.*<sup>135</sup> in the methacrylic acid system in which the initial temperature was lowered.

Spin modes have also been observed in the FP of transition metal nitrate acrylamide complexes,<sup>107,109</sup> which are solid, but were not observed in the frontal acrylamide polymerization system.<sup>99</sup>

The single-head spin mode was studied in detail by Ilyashenko and Pojman.<sup>136</sup> They were able to estimate the Zeldovich number by using data from the initiator and the methacrylic acid. The value at room temperature was about 7, less than the critical value for spin modes. In fact, fronts at room temperature were planar and spin modes only appeared by lowering the initial temperature. However, spin modes could be observed by increasing the heat loss from the reactor by immersing the tube in water or oil.

#### 4.38.5.16.5 Effect of complex kinetics

Solovoyov *et al.*<sup>137</sup> performed two-dimensional numerical simulations using a standard three-step free-radical mechanism. They calculated the Zeldovich number from the overall activation energy using the steady-state theory and determined the

critical values for bifurcations to periodic modes and found that the complex kinetics stabilized the front.

Shult and Volpert<sup>138</sup> performed the linear stability analysis for the same model and confirmed this result. Spade and Volpert<sup>139</sup> studied linear stability for nonadiabatic systems. Gross and Volpert<sup>140</sup> performed a nonlinear stability for the one-dimensional case. Commissiong *et al.*<sup>141</sup> extended the nonlinear analysis to two dimensions. They confirmed that, unlike in SHS,<sup>142</sup> uniform pulsations are difficult to observe in FP. In fact, no such one-dimensional pulsating modes have been observed.

An interesting problem arises in the study of fronts with multifunctional acrylates. At room temperature, acrylate like 1,6-hexanediol diacrylate (HDDA) and TGDMA exhibit spin modes. In fact, if an inert diluent, such as DMSO is added, the spin modes are more apparent even though the front temperature is reduced. Masere and Pojman<sup>143</sup> found spin modes in the FP of a diacrylate at ambient conditions. Thus, although the mechanical quality of the resultant polymer material can be improved by using multifunctional acrylates, spin modes may appear and a nonuniform product results. This observation implicates the role of polymer crosslinking in front dynamics. In that same work, Masere and Pojman showed that pH indicators could be added to act as dyes that were bleached by the free radicals, making the observation of the spin pattern readily apparent (Figure 31).



**Figure 31** A single-head spin mode propagating around a front of 1,6-hexanediol diacrylate (40%) in diethyl phthalate with Luperox 231 as the initiator.<sup>144</sup> Tube diameter was 1.5 cm.

Tryson and Schultz<sup>145</sup> studied the energy of activation of photopolymerized multifunctional acrylates and found it increased with increasing conversion because of crosslinking. Gray found that the energy of activation of HDDA increased exponentially during the reaction.<sup>146</sup> Applying the steady-state theory of polymerization to Gray's results, Masere *et al.*<sup>144</sup> calculated the effective energy of activation for thermally initiated polymerization (photoinitiation has no energy of activation) by including the energy of activation of a typical peroxide. They calculated that the energy of activation of HDDA polymerization increased from  $80 \text{ kJ mol}^{-1}$  at 0% conversion, the same as methacrylic acid, to a  $140 \text{ kJ mol}^{-1}$  at 80% conversion. This can explain how spin modes appear at room temperature with multifunctional acrylates but not monoacrylates. The Zeldovich number of methacrylic acid polymerization at room temperature is below the stability threshold. Using the activation energy at the highest conversion that can be obtained with HDDA, Masere *et al.* estimated a Zeldovich number of 12.

Masere *et al.*<sup>144</sup> studied fronts with a peroxide initiator at room temperature and used two bifurcation parameters. They added an inert diluent, diethyl phthalate, to change the front temperature and observed a variety of modes. More interestingly, they also varied the ratio of a monoacrylate, benzyl acrylate, to HDDA, keeping the front temperature constant. Changing the extent of crosslinking changed the effective energy of activation, which revealed a wide array of interesting spin modes. Using trimethylol propane triacrylate in DMSO, they observed complex modes (Figure 32).

The three-dimensional nature of the helical pattern was studied by Manz *et al.*<sup>147</sup> using Magnetic Resonance Imaging (MRI). Pojman *et al.* observed zigzag modes in square reactors<sup>148</sup> and bistability in conical reactors.<sup>149</sup>

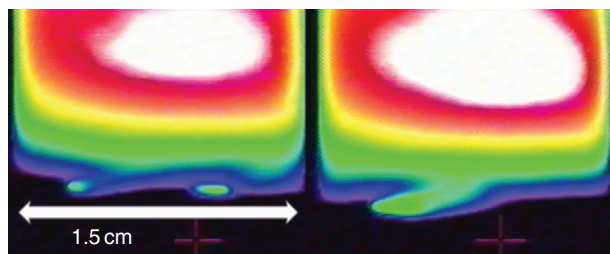


**Figure 32** Complex modes of propagation observed with an IR camera in a 1.5 cm tube with trimethylol propane triacrylate in DMSO with Luperox 231.

#### 4.38.5.16.6 Effect of bubbles

Pojman *et al.*<sup>135</sup> found an unusual mode of propagation when there are large amounts of very small bubbles that can occur when a linear polymer precipitates from its monomer. In studying fronts of methacrylic acid polymerization, they observed convection that periodically occurred under the front at the same time as the front deformed and undulated. The period of convection was about 20 s and remained constant during the entire front propagation.

Volpert *et al.*<sup>150</sup> analyzed the effect of the thermal expansion of the monomer on the thermal stability and concluded that the reaction front becomes less stable than without thermal expansion. The effective thermal expansion can be increased because of the bubbles, and it can considerably affect the stability conditions.

#### 4.38.5.16.7 Effect of buoyancy

The first experimental confirmation that gravity plays a role in spin modes in a liquid–solid system came in the study of descending fronts in which the viscosity was significantly increased with silica gel. Masere *et al.*<sup>144</sup> found that silica gel significantly altered the spin behavior, as predicted by Garbey *et al.*<sup>116</sup> Pojman *et al.*<sup>148</sup> made a similar observation in square reactors. Pojman *et al.*<sup>79</sup> studied the dependence of spin modes on viscosity with the FP of HDDA with persulfate initiator. They found that the number of spins was independent of the viscosity until a critical viscosity was reached, when the spins vanished.

The issues arises why the analysis of Ilyashenko and Pojman worked so well for the methacrylic acid system, even though they did not consider the effect of convection. They induced spin modes by reducing the initial temperature to  $0 \text{ }^\circ\text{C}$  – below the melting point of methacrylic acid. Thus, the system was a solid–solid system and so hydrodynamics played only a small role.

McFarland *et al.*<sup>151,152</sup> observed that spin modes did not occur when the initiator was microencapsulated. Not only were spin modes not observed, the material was 10 times stronger, which the authors attributed to the absence of spin modes.

#### 4.38.5.16.8 Three-dimensional frontal polymerization

FP allows the study of spherically propagating fronts. Binici *et al.*<sup>153</sup> developed a system that was a gel created by the base-catalyzed reaction of a trithiol with a triacrylate. The gel was necessary to suppress convection. However, it turned out to be difficult to find a system that would exhibit spin modes in a gel. They succeeded and were able to create waves on the surface of the expanding polymerization front (Figure 33).

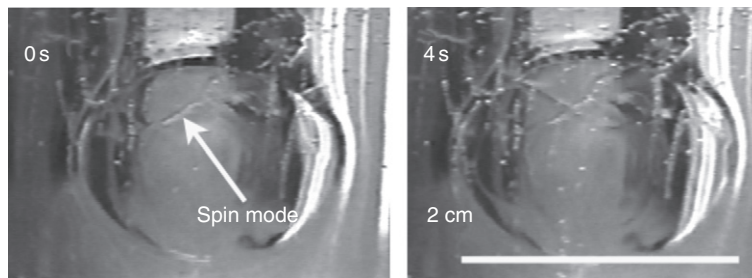


**Figure 33** A spin mode on the surface of a spherically expanding front of triacrylate polymerization. Adapted from Binici, B.; Fortenberry, D. I.; Leard, K. C.; *et al. J. Polym. Sci. Part A: Polym. Chem.* **2006**, *44*, 1387–1395.<sup>153</sup>

#### 4.38.5.17 The Effect of Fillers

Fillers are added to frontal systems to prevent convection, to modify the rheology of the unreacted formulation and to affect the mechanical properties of the product. Nason *et al.*<sup>154</sup> studied the effect of inorganic fillers on the photoinduced FP of a triacrylate. Not surprisingly, the front velocity decreased with increased loading of calcium carbonate or kaolin clay.

Pojman *et al.*<sup>155</sup> developed a system for studying Snell's Law of refraction in FP. Using trimethylolpropane triacrylate with 47% by mass kaolin clay (Polygloss 90), they created a formulation with the consistency of a putty, which could be molded into desired shapes. Viner *et al.*<sup>156</sup> used fillers that were inert but melted, so-called 'phase change materials', in an attempt to lower the front temperature without significantly reducing the front velocity.

Fumed silica was used by Bowden *et al.*<sup>119</sup> and McCaughey *et al.*<sup>120</sup> to precisely control the viscosity for convection studies. For acrylates, about 4 phr fumed silica will create a gel. For kaolin clay, about 40 phr is necessary to create moldable putty.

#### 4.38.5.18 Encapsulation of Initiators

McFarland *et al.*<sup>151,152</sup> studied the effect of encapsulating the initiator cumene hydroperoxide. They found that the front velocity was consistently slower than when the peroxide was dissolved. However, the particles do not need to be extremely small. The front velocity is 25% slower for 400- $\mu\text{m}$  capsules than for fronts with a dissolved initiator but almost the same with 50- $\mu\text{m}$  capsules. These systems hold the promise of creating fronts that propagate rapidly at moderate temperatures by coupling the encapsulated initiator with a redox system (Figure 34).

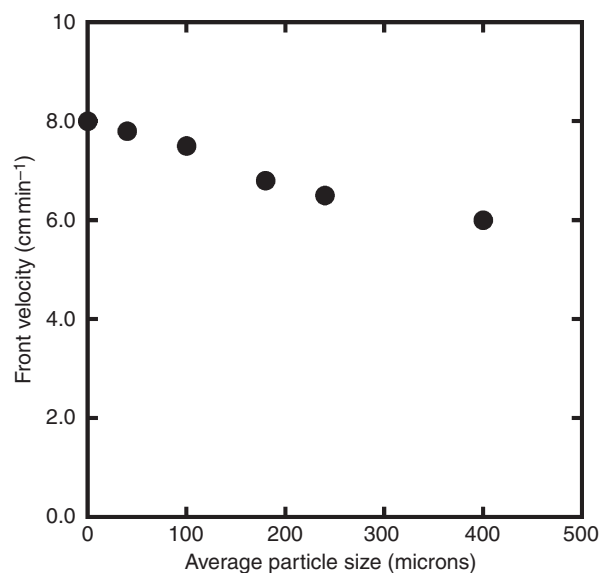


**Figure 34** The frontal polymerization velocity for TMPTA polymerization with encapsulated dicumyl peroxide. Image courtesy of Chris Bounds.

#### 4.38.5.19 Copolymerizations

Tredici *et al.*<sup>113</sup> studied the frontal copolymerization of acrylic acid–methacrylic acid, methyl methacrylate–methacrylic acid and styrene–methacrylic acid. They studied the velocity dependence on initiator concentration. They claimed that the elevated temperature of the front created a more random copolymer because the reactivity ratios were closer to one than under typical polymerization conditions. They performed numerical simulations for the velocity dependence and conversion on initiator concentration but strangely neither in experiments nor simulations did they study any dependence on monomer feed ratios.

Perry *et al.*<sup>157</sup> did study front velocity as a function of the monomer feed composition and the reactivity ratios. Frontal copolymerization experiments were performed with three different monomer systems. They are (1) methacrylic acid and acrylic acid (MAA-AA), (2) acryloyloxyethyltrimethylammonium chloride and acrylamide (AETMA-acrylamide), and (3) acrylic acid and acrylamide (AA-acrylamide). They chose these pairs because of their different reactivity ratios. The most significant result they found was that adding a highly reactive monomer could significantly increase the front velocity for a system that would propagate slowly or not at all. For example, AETMA in water would not support FP but could frontally copolymerize with acrylamide. For methacrylic acid, the velocity increased (from 2  $\text{cm min}^{-1}$ ) with 40% MAA to 4  $\text{cm min}^{-1}$  at 10% MAA.

Thiols can be used in two ways with free-radical polymerization.<sup>158</sup> Thiols react with electron-rich enes (allyl ethers) via a step-growth mechanism to create a polymer only if both ene and thiol have functionalities of at least two. The allyl ethers cannot homopolymerize. If thiols are present, the acrylate can homopolymerize and copolymerize with the thiol.<sup>159</sup> Pojman *et al.*<sup>160</sup> studied frontal thiol-ene polymerization using pentaerythritoltriallyl ether (PTE) and trimethylolpropanetrakis(3-mercaptopropionate) (95%) (TT1). Not surprisingly, the front velocity was a maximum at a 1:1 thiol:ene ratio (Figure 35).<sup>161</sup>

#### 4.38.5.20 Atom Transfer Radical Polymerization

Bidali *et al.*<sup>162</sup> performed frontal atom transfer radical polymerization (ATRP) with tri(ethylene glycol dimethacrylate). They used  $\text{CBr}_4$ , tris(2-aminoethyl)amine, and  $\text{CuBr}$ . When the components were dissolved in the monomer, the solution was cooled to 0 °C to prevent bulk polymerization, which did not react for at least 3 h. Samples were heated to 25 °C before fronts were then initiated, which propagated with velocities of about 0.5  $\text{cm min}^{-1}$ . The major advantage of this system compared to a typical peroxide-based system was the lack of bubbles. However, because the system reacted relatively quickly at room temperature, the system has limited applicability.

#### 4.38.5.21 Ring-Opening Metathesis Polymerization

Mariani *et al.*<sup>163</sup> first demonstrated that FP could be achieved with the ring-opening metathesis polymerization (ROMP) of dicyclopentadiene. In a typical run, a glass test tube already containing suitable amounts of solid Grubbs catalyst (GC) and  $\text{PPh}_3$  was filled with liquid dicyclopentadiene at 35 °C. After the reagents dissolved, the reaction mixture was cooled to 27 °C in order to permit solidification of the solution.

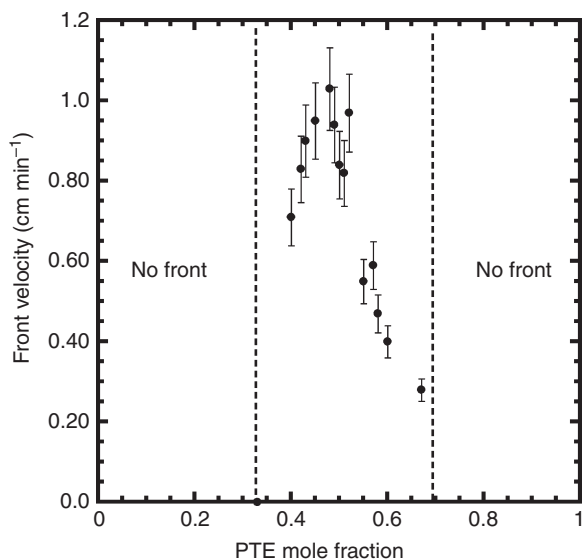


**Figure 35** The front velocity as a function of the mole ratio between pentaerythritoltriallyl ether (PTE) and trimethylolpropanetris(3-mercaptopropionate). Adapted from Pojman, J. A.; Varisli, B.; Perryman, A.; *et al. Macromolecules* **2004**, *37*, 691–693.<sup>160</sup>

A problem with this system is that it has a relatively short pot life. The authors found that by using  $\text{PPh}_3$  the pot life was extended to 20 min. To overcome this drawback, they dissolved all components at 35 °C and quickly cooled them to 27 °C. This means that frontal ring opening metathesis polymerization runs were performed on solid mixtures, which melted immediately before being reached by the front. If stored at 7–8 °C, the samples could support a front after 3 weeks.

#### 4.38.5.22 Polyurethanes

Fiori *et al.*<sup>164,165</sup> were the first to perform frontal urethane polymerization. They used 1,6-hexamethylene diisocyanate, ethylene glycol, and the catalyst dibutyltin dilaurate in DMSO with fumed silica. Pyrocatechol was added to extend the pot life up to 25 min (Figure 36). The front velocities were less than 1  $\text{cm min}^{-1}$ .

Texter and Ziemer<sup>166</sup> created polyurethanes via FP in micro-emulsions. Chen *et al.*<sup>167</sup> created epoxy-polyurethane hybrid networks frontally. Pot lives were on the order of hours. Hu *et al.*<sup>168</sup> frontally prepared urethane-acrylate copolymers in DMSO using persulfate as the initiator. Chen *et al.*<sup>92</sup> studied FP of poly(propylene oxide) glycol, 2,4-toluene diisocyanate, and 1,4-butanediol with the catalyst stannous caprylate in dimethylbenzene. At room temperature, bulk polymerization did not occur quickly, and the pot life could be extended to 6 h if the solution was cooled to 10 °C. Mariani *et al.*<sup>169</sup> prepared diurethane diacrylates.

#### 4.38.5.23 Epoxy Curing

In 1975, Arutiunian demonstrated frontal epoxy curing with amines using resins based on bisphenol A.<sup>170</sup> Chekanov *et al.*<sup>171</sup> studied the frontal curing of diglycidyl ether of bisphenol F (DGEBF), which was cured by the aliphatic amine curing agent Epicure 3371 in a stoichiometric ratio both frontally and in a batch-cure schedule. The pot life for the system was about

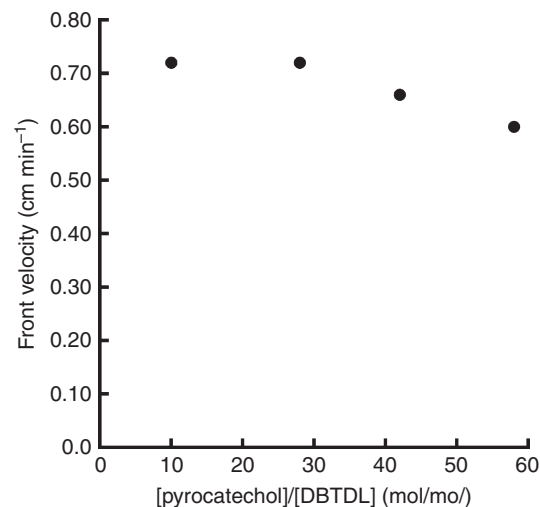


**Figure 36** Front velocity vs [pyrocatechol]/[DBTDL] ratio. Experimental conditions:  $[\text{DBTDL}]/[\text{HDI}] = 9.4 \times 10^{-4} \text{ mol mol}^{-1}$ , DMSO = 18 wt.%, Cabosil = 3 wt.%. Adapted from Fiori, S.; Mariani, A.; Ricco, L.; Russo, S. *Macromolecules* **2003**, *36*, 2674–2679.<sup>164</sup>

60 min. Glass transition temperatures ( $T_g$ ) were determined using differential scanning calorimetry (DSC) and dynamic mechanical analysis (DMA). The properties of the frontally cured epoxy resin were found to be very close to that of batch-cured epoxy resin. They achieved 90% of the mechanical strength in 10% of the time for a sample 2.2 cm in diameter by 25 cm in length. The front temperatures were about 250 °C with front velocities of 4  $\text{cm min}^{-1}$ . The maximum percentage of filler in the epoxy resin allowing propagation was 30%. Frulloni *et al.*<sup>172</sup> and Mariani *et al.*<sup>173</sup> studied a similar system and developed a phenomenological model of the front propagation.

Because the reaction between the amine curing agent and the epoxy is stoichiometric, the front velocity cannot be varied by changing the amount of curing agent without significantly affecting the conversion and mechanical properties of the product. Another significant difference between these systems and free-radical cured fronts is the relatively short pot life.

Mariani *et al.* combined FP and radical-induced cationic polymerization to cure thick samples of an epoxy monomer bleached by UV light. They used 3,4-Epoxy cyclohexylmethyl-3',4'-epoxycyclohexanecarboxylate (CE), benzoyl peroxide (BPO), and {4-[(2-hydroxytetradecyl)oxy]phenyl}phenyliodonium hexafluoroantimonate (HOPH). The effect of the relative amounts of cationic photoinitiator and radical initiator was investigated and was related to the front's velocity and its maximum temperature.

Scognamillo *et al.*<sup>174</sup> studied the cationic curing of a triepoxy using latent  $\text{BF}_3$ -amine catalysts.

#### 4.38.5.24 Binary Systems

If two noninteracting polymerization systems are mixed together, a binary FP can be created. Pojman *et al.*<sup>175,176</sup> studied the binary system composed of triethyleneglycol dimethacrylate with Luperox 231 as the free-radical initiator and diglycidyl ether of bisphenol A (DGEBA II), using the dual curing system

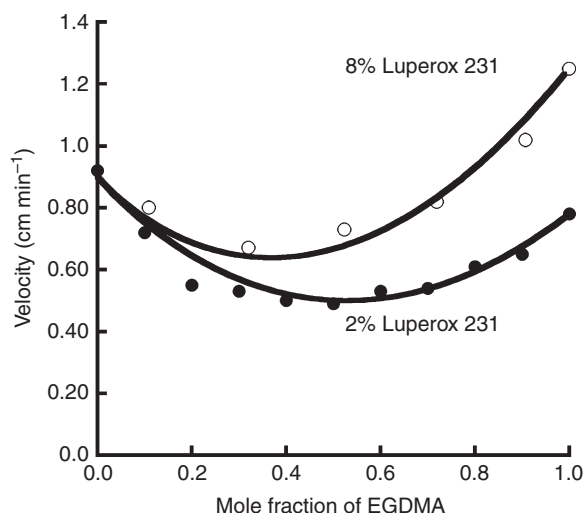


**Figure 37** The front velocity as a function of the ethyleneglycol dimethacrylate mole fraction in the binary frontal polymerization with diglycidyl ether of bisphenol F. Adapted from Pojman, J. A.; Griffith, J.; Nichols, H. A. *e-Polymers* **2004**, *13*, 1–7.<sup>176</sup>

of an alkyl amine (Epicure 3271) and a boron trichloride/amine (BC13-NR3). **Figure 37** shows how the front velocity exhibits a minimum as a function of the mole fraction of the two reactants.

#### 4.38.5.25 Patents

In 1980, Dixon<sup>177</sup> received the first patent on FP, entitled *In Depth Curing of Resins Induced by UV Radiation*. He produced curing to depths of 500 mils (500/1000 in.) using a combination of a photoinitiator, thermal initiator, and multifunctional acrylate resin. The UV light caused a photopolymerization on the surface, which then triggered a propagating front. To increase the reactivity, he also added an accelerator such as a tertiary amine.

Scranton *et al.*<sup>178</sup> patented *Thick, Composite Parts Made from Photopolymerizable Compositions and Methods for Making Such Parts*, in which photopolymerization was combined with thermal FP.

In 2000 and 2001, Pojman and McCardle<sup>179,180</sup> received two patents on *Functionally Gradient Polymeric Materials*. Functionally gradient materials possess spatially varying properties. By creating an ascending front into which reagents were flowed at a rate sufficient to maintain a layer thin enough to significantly reduce buoyancy-driven convection, spatial variations of properties could be created. Chekanov and Pojman<sup>181</sup> discussed the process in detail.

Pfeil *et al.*<sup>182</sup> received a patent in 2003 on *Mortar Composition, Curable by Frontal Polymerization, and a Method for Fastening Tie Bars*. Chemical anchors are adhesives, usually based on epoxy chemistry that are used to secure rods in holes drilled in concrete. Their approach is to use multifunctional acrylates with silica and quartz fillers and thermal initiators as the frontally cured chemical anchor.

Bürgel and Böck<sup>183</sup> patented a further development in chemical anchors. They used a two-part formulation with one consisting of a monomer with an organic substituted

ammonium salt and the other consisting of the monomer with ammonium persulfate. When the two components are mixed, the organic substituted ammonium salt exchanges with the ammonium persulfate to form an organic soluble persulfate, which does not produce gas during decomposition.

Gregory<sup>184</sup> patented *Ultraviolet Curable Resin Compositions Having Enhanced Shadow Curing Properties* in 2001. This patent has the same idea as Dixon's patent, that is, use photopolymerization at the surface of a filled resin to trigger a thermal front. Gregory went beyond using peroxide-cured vinyl resins. He used dialkyl iodonium salts, sensitized by  $\alpha$ -hydroxy ketones, that produced Lewis acids upon UV irradiation. The Lewis acid triggered cationic polymerization of epoxy resins and vinyl ethers. The heat from the photoinitiated process decomposes peroxides into radicals that react with the iodonium salts to produce Lewis acids.

Crivello<sup>185</sup> patented *Command-Cure Adhesive* that is activated by UV light and then propagates thermally.

Pojman *et al.*<sup>186</sup> have a patent pending on FP microencapsulated monomers.

#### 4.38.5.26 Applications of Thermal Frontal Polymerization

These patents demonstrate some possible applications of thermal FP but none have been commercialized. So we now consider if FP is more than a laboratory curiosity or an interesting way to study nonlinear phenomena in polymeric systems.

##### 4.38.5.26.1 Solventless processing

The ability to prepare thermoplastics rapidly without solvent is a potential advantage.<sup>54,95,187–190</sup> Two problems were present in all these works, namely, lack of complete conversion and the necessity to add a component to suppress convection.

##### 4.38.5.26.2 Energy savings

Numerous early publications included the claim that FP required less energy than conventional processing methods.<sup>53,56</sup> This was based on the observation that once the reaction was begun, no additional energy input was required. However, no detailed energy balance has been performed to verify this claim. Moreover, unless the conversion of a monofunctional monomer is 100%, some purification is required, which would reduce the energy advantage.

##### 4.38.5.26.3 Rapid synthesis of materials

For all of the chemistries studied, a clear advantage over bulk polymerization is the speed at which materials can be prepared. The high temperature increases the rate of reaction but because that reaction is localized, the process can be carried out safely. For monoacrylates, the high temperature leads to relatively low molecular weights but this may be acceptable for some applications.

##### 4.38.5.26.4 Preparation of hydrogels

Frontal preparation of hydrogels is a promising area. The first example was performed by Washington and Steinbock in 2001 with *N*-isopropylacrylamide.<sup>191</sup> They were able to make a polymer with the expected temperature-dependent properties but in much less time than with a batch polymerization.

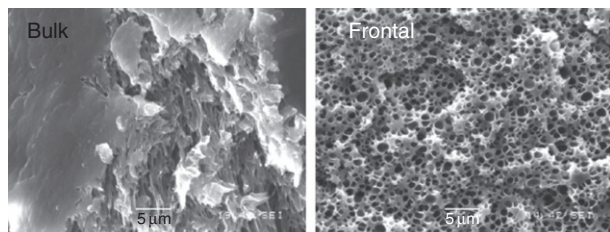


**Figure 38** A comparison of porous polyacrylamide prepared by bulk polymerization and by frontal polymerization. Adapted from Lu, G. D.; Yan, Q. Z.; Ge, C. C. *Polym. Int.* **2007**, *56*, 1016–1020.<sup>192</sup>

Lu *et al.*<sup>192</sup> shows that porous polyacrylamide could be prepared frontally using  $\text{NaHCO}_3$  as a foaming agent. The frontal samples (**Figure 38**) exhibited higher swelling rate and swelling ratio than the bulk polymerized samples. Pujari *et al.*<sup>193</sup> studied a series of glycidyl methacrylate-ethylene dimethacrylate copolymers synthesized by FP and by dispersion polymerization. They found that the frontal samples had higher internal pore volume and surface area than those prepared by dispersion polymerization but they had inferior surface morphologies.

Tu *et al.*<sup>194</sup> prepared amphiphilic gels in *N*-methyl-2-pyrrolidone as the solvent. They found the gels had good swelling capacity in water and organic solvents but could be prepared more rapidly than via bulk polymerization. Fang *et al.*<sup>195</sup> frontally prepared *N*-vinyl pyrrolidinone-based thermosensitive hydrogels in glycerol. Feng *et al.*<sup>196</sup> prepared macroporous polyacrylamide and poly(*N*-isopropylacrylamide) monoliths using FP.

Yan *et al.*<sup>197–199</sup> studied the FP of starch-grafted hydrogels. They used partially neutralized acrylic acid in water containing starch and bisacrylamide with persulfate as the initiator and determined that they hydrogels produced were spatially homogeneous.

All the investigators Mariani and his co-workers prepared poly(*N,N*-dimethylacrylamide) hydrogels<sup>91</sup> and super water absorbent hydrogels frontally.<sup>200</sup> Gavini *et al.*<sup>89</sup> evaluated FP to prepare drug controlled release systems based on polyacrylamide. They tested the sodium salt of diclofenac as the drug to

be released and found that it survived the FP process. They also found that the samples showed comparable drug release characteristics to those of the batch polymerized samples.

#### 4.38.5.26.5 Consolidation of stone

Proietti *et al.*,<sup>201</sup> Mariani *et al.*,<sup>202</sup> and Vicini *et al.*<sup>203</sup> have studied FP to consolidate stone. The idea is to allow an acrylate-initiator solution to infuse into a stone structure and then start a front to cure the monomer. The advantage over two-part formulations is that the resin would have a long time to infuse before curing. The advantage over autoclave curing is the material can be prepared in place and not moved to a lab.

#### 4.38.5.26.6 Autoclaveless curing of large composites

White explored the idea of using the frontal curing of large composite parts as a means to avoid the charring that can occur when heat released from the curing causing a thermal runaway.<sup>204,205</sup> This approach is worth further exploration.

#### 4.38.5.26.7 Cure-on-demand repair and adhesives

A promising application of FP is cure-on-demand repair and adhesives. The concept is to use a system with a very long pot life that can be used as a putty to fill a hole (**Figure 39**) in a floor, wall, or wood, which can be locally heated to start a front that rapidly cures the resin. The approach can also be applied to creating a wood adhesive. It would be especially exciting if it could be applied to the rapid repair of composites.

### 4.38.6 Conclusions

The three modes of FP have proven to offer advantages for different applications. Photofrontal polymerization is driven by a continuous flux of energy and has been applied to the preparation of microfluidic chips. It can be applied to any photopolymerization. IFP relies on the gel effect to create a slowly moving localized polymerization through monomers like methyl methacrylate. This method can be used to prepare gradient refractive index materials.

Thermal frontal polymerization can be applied to the widest range of materials. Any polymerization that follows



**Figure 39** Cure-on-demand repair of a stone floor using an acrylate-based putty filled with kaolin. The coin is a US quarter.

Arrhenius kinetics and is highly exothermic can support localized polymerizations that propagate. Frontal polymerization has been studied with many different polymerization mechanisms but free-radical polymerization is the most studied. Most of the work has focused on the dynamics of the process, but recently applications have been studied. Hydrogels have been prepared frontally, which have superior properties to those prepared by conventional methods.

The major advantage of thermal frontal polymerization is the high rate of conversion. Cure-on-demand applications appear to be the most promising use for this approach.

## References

- Pearlstein, A. J. *J. Phys. Chem.* **1985**, *89*, 1054–1058.
- Pearlstein, A. J.; Harris, R. M.; Terronesq, G. *J. Fluid. Mech.* **1989**, *202*, 443–465.
- Terrones, G.; Pearlstein, A. J. *Phys. Fluids A* **1989**, *1*, 845–853.
- Briskman, V. A. In *Polymer Research in Microgravity: Polymerization and Processing*; Downey, J. P.; Pojman, J. A., Eds.; ACS Symposium Series No. 793; American Chemical Society: Washington, DC, 2001; pp 97–110.
- Terrones, G.; Pearlstein, A. J. *Macromolecules* **2001**, *34*, 3195–3204.
- Terrones, G.; Pearlstein, A. J. *Macromolecules* **2004**, *37*, 1565–1575.
- Cabral, J. T.; Hudson, S. D.; Harrison, C.; Douglas, J. F. *Langmuir* **2004**, *20*, 10020–10029.
- Koike, Y.; Hatanaka, H.; Otsuka, Y. *Appl. Opt.* **1984**, *23*, 1779–1783.
- Ohtsuka, Y.; Koike, Y. *Appl. Opt.* **1984**, *23*, 1774–1778.
- Righetti, P. G.; Bossi, A.; Giglio, M.; et al. *Electrophoresis* **1994**, *15*, 1005–1013.
- Warren, J. A.; Cabral, J. T.; Douglas, J. F. *Phys. Rev. E* **2005**, *72*, 021801.
- Norrish, R. G. W.; Smith, R. R. *Nature* **1942**, *150*, 336–337.
- Trommsdorff, E.; Köhle, H.; Lagally, P. *Makromol. Chem.* **1948**, *1*, 169–198.
- Koike, Y.; Takezawa, Y.; Ohtsuka, Y. *Appl. Opt.* **1988**, *27*, 486–491.
- Koike, Y.; Nihei, E.; Tanio, N.; Ohtsuka, Y. *Appl. Opt.* **1990**, *29*, 2686–2691.
- Koike, Y. *Polymer* **1991**, *32*, 1737–1745.
- Koike, Y. In *Polymers for Lightwave and Integrated Optics*; Hornak, L. A., Ed.; Marcel Dekker: New York, NY, 1992; pp 71–104.
- Koike, Y.; Nihei, E. U.S. Patent 5,253,323, 1993.
- Ishigure, T.; Nihei, E.; Koike, Y. *Appl. Opt.* **1994**, *33*, 4261–4266.
- Koike, Y.; Asakawa, A.; Wu, S. P.; Nihei, E. *Appl. Opt.* **1995**, *34*, 4669–4673.
- Sasaki, K.; Koike, Y. U.S. Patent 5,450,232, 1995.
- Wu, S. P.; Nihei, E.; Koike, Y. *Polymer J.* **1995**, *27*, 21–25.
- Nihei, E.; Ishigure, T.; Koike, Y. *Appl. Opt.* **1996**, *35*, 7085–7090.
- Tagaya, A.; Teramoto, S.; Nihei, E.; et al. *Appl. Opt.* **1997**, *36*, 572–578.
- Koike, Y.; Hidaka, H.; Ohtsuka, Y. *Appl. Opt.* **1985**, *24*, 4321–4325.
- Koike, Y.; Koike, K. *J. Polym. Sci. Part B: Polym. Phys.* **2011**, *49*, 2–17.
- Golubev, V. B.; Gromov, D. G.; Korolev, B. A. *J. Appl. Polym. Sci.* **1992**, *46*, 1501–1502.
- Gromov, D. G.; Frisch, H. L. *J. Appl. Polym. Sci.* **1992**, *46*, 1499–1500.
- Ivanov, V. V.; Stegno, E. V.; Pushchaeva, L. M. *Chem. Phys. Rep.* **1997**, *16*, 947–951.
- Ivanov, V. V.; Stegno, E. V.; Pushchaeva, L. M. *Polym. Sci. Ser. A* **2002**, *44*, 1017–1022.
- Lewis, L. L.; DeBisschop, C. A.; Pojman, J. A.; Volpert, V. A. In *Nonlinear Dynamics in Polymeric Systems*; Pojman, J. A.; Tran-Cong-Miyata, Q., Eds.; ACS Symposium Series No. 869; American Chemical Society: Washington, DC, 2003; pp 169–185.
- Lewis, L. L.; DeBisschop, C. S.; Pojman, J. A.; Volpert, V. A. *J. Polym. Sci. Part A Polym. Chem.* **2005**, *43*, 5774–5786.
- Lewis, L. L.; Massey, K. N.; Meyer, E. R.; et al. *Opt. Laser. Eng.* **2008**, *46*, 900–910.
- Evsratova, S. I.; Antrim, D.; Fillingane, C.; Pojman, J. A. *J. Polym. Sci. Part A: Polym. Chem.* **2006**, *44*, 3601–3608.
- Ohlemiller, T. J. *Prog. Energy Combust. Sci.* **1985**, *11*, 277–310.
- Spade, C. A.; Volpert, V. A. *Math. Comp. Model.* **1999**, *30*, 67–73.
- Spade, C. A.; Volpert, V. A. *Macromol. Theory Simul.* **2000**, *9*, 26–46.
- Schult, D. A.; Spade, C. A.; Volpert, V. A. *Appl. Math. Lett.* **2002**, *15*, 749–754.
- Masere, J.; Lewis, L. L.; Pojman, J. A. *J. Appl. Polym. Sci.* **2001**, *80*, 686–691.
- Masere, J.; Chekanov, Y.; Warren, J. R.; et al. *J. Polym. Sci. Part A: Polym. Chem.* **2000**, *38*, 3984–3990.
- Barelko, V. V.; Barkalov, I. M.; Goldanskii, V. I.; et al. *Adv. Chem. Phys.* **1988**, *74*, 339–385.
- Barelko, V. V.; Barkalov, I. M.; Kiryukhin, D. P. *Russ. Chem. Rev.* **1990**, *59*, 205–217.
- Kiryukhin, D. P.; Barelko, V. V.; Barkalov, I. M. *High Energy Chem.* **1999**, *33*, 133–144.
- Volodin, J. E.; Zvyagin, V. N.; Ivanova, A. N.; Barelko, V. V. *Adv. Chem. Phys.* **1990**, *77*, 551–606.
- Barelko, V. V.; Kiryukhin, D. P. *Russ. Chem. Rev.* **1994**, *63*, 491.
- Kiryukhin, D. P.; Barkalov, I. M. *Polym. Sci. Ser. B* **2000**, *42*, 244–253.
- Kiryukhin, D. P.; Barkalov, I. M. *Russ. Chem. Rev.* **2003**, *72*, 217–231.
- Kiryukhin, D. P.; Kichigina, G. A.; Barelko, V. V. *Polym. Sci. Ser. B* **2010**, *52*, 221–226.
- Chechilo, N. M.; Enikolopyan, N. S. *Dokl. Phys. Chem.* **1974**, *214*, 174–176.
- Chechilo, N. M.; Enikolopyan, N. S. *Dokl. Phys. Chem.* **1975**, *221*, 392–394.
- Chechilo, N. M.; Enikolopyan, N. S. *Dokl. Phys. Chem.* **1976**, *230*, 840–843.
- Chechilo, N. M.; Khvilivitskii, R. J.; Enikolopyan, N. S. *Dokl. Akad. Nauk SSSR* **1972**, *204*, 1180–1181.
- Davyan, S. P.; Zhirkov, P. V.; Vol'fson, S. A. *Russ. Chem. Rev.* **1984**, *53*, 150–163.
- Pojman, J. A. *J. Am. Chem. Soc.* **1991**, *113*, 6284–6286.
- Pojman, J. A.; Ilyashenko, V. M.; Khan, A. M. *J. Chem. Soc. Faraday Trans.* **1996**, *92*, 2825–2837.
- Khan, A. M.; Pojman, J. A. *Trends Polym. Sci. (Cambridge, U.K.)* **1996**, *4*, 253–257.
- Washington, R. P.; Steinbock, O. *Polym. News* **2003**, *28*, 303–310.
- Merzhanov, A. G.; Borovinskaya, I. P. *Dokl. Nauk SSSR* **1972**, *204*, 336–339.
- Merzhanov, A. G. *Archiv. Comb.* **1981**, *1*, 23.
- Varma, A.; Lebrat, J.-P. *Chem. Eng. Sci.* **1992**, *47*, 2179–2194.
- Puszynski, J.; Degreve, J.; Hlavacek, V. *Ind. Eng. Chem. Res.* **1987**, *26*, 1424–1434.
- Anselm-Tamburini, U.; Munir, Z. A. *J. Appl. Phys.* **1989**, *66*, 5039–5045.
- Merzhanov, A. G. *Int. J. SHS* **1993**, *2*, 113–157.
- Merzhanov, A. G. *Combust. Sci. Tech.* **1994**, *98*, 307–336.
- Dvoryankin, A. V.; Strunina, A. G.; Merzhanov, A. G. *Combust. Explos. Shock Waves* **1982**, *18*, 134–139.
- Merzhanov, A. G.; Dvoryankin, A. V.; Strunina, A. G. *Dokl. Phys. Chem.* **1982**, *267*, 869–872.
- Sivashinsky, G. I. *SIAM J. Appl. Math.* **1981**, *40*, 432–438.
- Volpert, A. I.; Volpert, V. A.; Volpert, V. A. *Traveling Wave Solutions of Parabolic Systems*; American Mathematical Society, Providence, RI, 1994.
- Strunin, D. V.; Strunina, A. G.; Rumanov, E. N.; Merzhanov, A. G. *Phys. Lett. A* **1994**, *192*, 361–363.
- Davyan, S. P.; Surkov, N. F.; Rozenberg, B. A.; Enikolopyan, N. S. *Dokl. Phys. Chem.* **1977**, *232*, 64–67.
- Zhizhin, G. V.; Segal, A. S. *Z. Prikl. Meh. Tehn. Fiz.* **1988**, 62–71.
- Babadzhanyan, A. S.; Volpert, V. A.; Volpert, V. A.; et al. *Combust. Explos. Shock Waves* **1988**, *24*, 711–719.
- Babadzhanyan, A. S.; Volpert, V. A.; Volpert, V. A.; et al. *Combust. Explos. Shock Waves* **1989**, *25*, 23–31.
- Megrabova, I. N.; Volpert, V. A.; Volpert, V. A.; Davtyan, S. P. *Dokl. Phys. Chem.* **1990**, *307*, 618–620.
- Megrabova, I. N.; Volpert, V. A.; Volpert, V. A.; Davtyan, S. P. *Combust. Explos. Shock Waves* **1991**, *26*, 413–417.
- Babadzhanyan, A. S.; Volpert, V. A.; Davtyan, S. P. *Dokl. Phys. Chem.* **1987**, *293*, 357–360.
- Zhizhin, G. V.; Segal, A. S.; Babadzhanyan, A. S.; et al. *Kinet. Katal.* **1986**, *27*, 1310–1314.
- Solov'yov, S. E.; Volpert, V. A.; Davtyan, S. P. *SIAM J. Appl. Math.* **1993**, *53*, 907–914.
- Pojman, J. A.; Popwell, S.; Fortenberry, D. I.; et al. In *Nonlinear Dynamics in Polymeric Systems*; Pojman, J. A.; Tran-Cong-Miyata, Q., Eds.; ACS Symposium Series No. 869; American Chemical Society: Washington, DC, 2003; pp 106–120.
- Pojman, J. A.; Tran-Cong-Miyata, Q. Eds. *Nonlinear Dynamics with Polymers: Fundamentals, Methods and Applications*; Wiley-VCH Verlag GmbH & Co KGaA: Weinheim, Germany, 2010.
- Ritter, I. R.; Olmstead, W. E.; Volpert, V. A. *SIAM J. Appl. Math.* **2003**, *63*, 1831–1848.
- Heifetz, A.; Ritter, L. R.; Olmstead, W. E.; Volpert, V. A. *Math. Comput. Model.* **2005**, *41*, 271–285.
- Nason, C.; Roper, T.; Hoyle, C.; Pojman, J. A. *Macromolecules* **2005**, *38*, 5506–5512.
- Pojman, J. A.; Willis, J.; Fortenberry, D.; et al. *J. Polym. Sci. Part A: Polym. Chem.* **1995**, *33*, 643–652.
- Pojman, J. A.; Khan, A. M.; West, W. *Polym. Prepr. (Am Chem. Soc. Div. Polym. Chem.)* **1992**, *33*, 1188–1189.

86. Pojman, J. A.; Craven, R.; Khan, A.; West, W. J. *Phys. Chem.* **1992**, *96*, 7466–7472.
87. Nagy, I. P.; Pojman, J. A. *J. Phys. Chem.* **1996**, *100*, 3299–3304.
88. Pojman, J. A.; Curtis, G.; Ilyashenko, V. M. *J. Am. Chem. Soc.* **1996**, *118*, 3783–3784.
89. Gavini, E.; Mariani, A.; Rassu, G.; et al. *Eur. Polym. J.* **2009**, *45*, 690–699.
90. Alzari, V.; Mariani, A.; Monticelli, O.; et al. *J. Polym. Sci. Part A: Polym. Chem.* **2010**, *48*, 5375–5381.
91. Caria, G.; Alzari, V.; Monticelli, O.; et al. *J. Polym. Sci. Part A: Polym. Chem.* **2009**, *47*, 1422–1428.
92. Chen, S. H.; Sui, J.; Chen, L. *Colloid Polym. Sci.* **2005**, *283*, 932–936.
93. Khanukaev, B. B.; Kozhushner, M. A.; Enikolopyan, N. S. *Combust. Explos. Shock Waves* **1974**, *10*, 562–568.
94. Khanukaev, B. B.; Kozhushner, M. A.; Enikolopyan, N. S. *Dokl. Phys. Chem.* **1974**, *214*, 84–87.
95. Goldfeder, P. M.; Volpert, V. A.; Ilyashenko, V. M.; et al. *J. Phys. Chem. B* **1997**, *101*, 3474–3482.
96. Pojman, J. A.; Nagy, I. P.; Salter, C. J. *Am. Chem. Soc.* **1993**, *115*, 11044–11045.
97. Siggia, S.; Hanna, J. G. *Quantitative Organic Analysis Via Functional Groups*; Wiley: New York, NY, 1979.
98. Kolthoff, I. M.; Sandell, E. B.; Meehan, E. J.; Bruckenstein, S. *Quantitative Chemical Analysis*; Macmillan: London, UK, 1969; pp 842–847.
99. Fortenberry, D. I.; Pojman, J. A. *J. Polym. Sci. Part A: Polym. Chem.* **2000**, *38*, 1129–1135.
100. Pojman, J. A.; Willis, J. R.; Khan, A. M.; West, W. W. *J. Polym. Sci. Part A: Polym. Chem.* **1996**, *34*, 991–995.
101. Sówka, E.; Leonowicz, M.; Kaźmierczak, J.; et al. *Physica B* **2006**, *384*, 282–285.
102. Kholpanov, L. P.; Zakiev, S. E.; Pomogailo, A. D. *Polym. Sci. Ser. A* **2006**, *48*, 11–17.
103. Pomogailo, A. D.; Dzhardimalieva, G. I. *Polym. Sci. Ser. A* **2004**, *46*, 250–263.
104. Kholpanov, L. P.; Zakiev, S. E.; Pomogailo, A. D. *Dokl. Phys. Chem.* **2004**, *395*, 84–87.
105. Dzhardimalieva, G. I.; Golubeva, N. D.; Pomogailo, A. D. *Diffus. Defect Data Pt. B* **2003**, *94*, 323–328.
106. Dzhardimalieva, G. I.; Pomogailo, A. D.; Volpert, V. A. *J. Inorg. Organomet. Polym.* **2002**, *12*, 1–21.
107. Barelko, V. V.; Pomogailo, A. D.; Dzhardimalieva, G. I.; et al. *Chaos* **1999**, *9*, 342–347.
108. Pomogailo, A. D.; Savostyanov, V. S.; Dzhardimalieva, G. I.; et al. *Russ. Chem. Bull.* **1995**, *44*, 1056–1061.
109. Savostyanov, V. S.; Kritskaya, D. A.; Ponomarev, A. N.; Pomogailo, A. D. *J. Polym. Sci. Part A: Polym. Chem.* **1994**, *32*, 1201–1212.
110. Mariani, A.; Nuvoli, D.; Alzari, V.; Pini, M. *Macromolecules* **2008**, *41*, 5191–5196.
111. Enikolopyan, N. S.; Kozhushner, M. A.; Khanukaev, B. B. *Dokl. Phys. Chem.* **1974**, *217*, 676–678.
112. Pojman, J. A.; Khan, A. M.; Mathias, L. J. *Microgravity Sci. Technol.* **1997**, *X*, 36–40.
113. Tredici, A.; Pecchini, R.; Morbidelli, M. *J. Polym. Sci. Part A: Polym. Chem.* **1998**, *36*, 1117–1126.
114. Sawada, H. *Thermodynamics of Polymerization*; Marcel Dekker: New York, NY, 1976.
115. Odian, G. *Principles of Polymerization*, 4th ed.; Wiley: New York, NY, 2004.
116. Garbey, M.; Taik, A.; Volpert, V. *Quart. Appl. Math.* **1998**, *56*, 1–35.
117. Garbey, M.; Taik, A.; Volpert, V. *Prepr. CNRS* **1994**, *187*, 1–42.
118. Garbey, M.; Taik, A.; Volpert, V. *Quart. Appl. Math.* **1996**, *54*, 225–247.
119. Bowden, G.; Garbey, M.; Ilyashenko, V. M.; et al. *J. Phys. Chem. B* **1997**, *101*, 678–686.
120. McCaughey, B.; Pojman, J. A.; Simmons, C.; Volpert, V. A. *Chaos* **1998**, *8*, 520–529.
121. Bazile, M., Jr.; Nichols, H. A.; Pojman, J. A.; Volpert, V. J. *Polym. Sci. Part A: Polym. Chem.* **2002**, *40*, 3504–3508.
122. Bidali, S.; Ducrot, A.; Mariani, A.; Rustici, M. *e-Polymers* **2004**, *44*, 1–20.
123. Pojman, J. A.; Gunn, G.; Owens, J.; Simmons, C. *J. Phys. Chem. Part B* **1998**, *102*, 3927–3929.
124. Texier-Picard, R.; Pojman, J. A.; Volpert, V. A. *Chaos* **2000**, *10*, 224–230.
125. Pojman, J. A.; Epstein, I. R. *J. Phys. Chem.* **1990**, *94*, 4966–4972.
126. Pojman, J. A.; Epstein, I. R.; Karni, Y.; Bar-Ziv, E. *J. Phys. Chem.* **1991**, *95*, 3017–3021.
127. Ostrach, S. *Annu. Rev. Fluid Mech.* **1982**, *14*, 313–345.
128. Asakura, K.; Nihei, E.; Harasawa, H.; et al. In *Nonlinear Dynamics in Polymeric Systems*; Pojman, J. A.; Tran-Cong-Miyata, Q., Eds.; ACS Symposium Series No. 869; American Chemical Society: Washington, DC, 2003; pp 135–146.
129. Gusika, P. L. *Khim. Fiz.* **1982**, *7*, 988–993.
130. Maksimov, Y. M.; Pak, A. T.; Lavrenchuk, G. V.; et al. *Comb. Expl. Shock Waves* **1979**, *15*, 415–418.
131. Pojman, J. A. In *Chemomechanical Instabilities in Responsive Materials (NATO Science for Peace and Security Series A: Chemistry and Biology)*; Borckmans, P.; De Kepper, P.; Khokhlov, A. R.; Métais, S., Eds.; Springer: Dordrecht, The Netherlands, 2009; pp 221–240.
132. Pojman, J. A. In *Nonlinear Dynamics with Polymers: Fundamentals, Methods and Applications*; Pojman, J. A.; Tran-Cong-Miyata, Q., Eds.; Wiley-VCH Verlag GmbH & Co. KGaA: Weinheim, Germany, 2010; pp 45–68.
133. Begishev, V. P.; Volpert, V. A.; Davtyan, S. P.; Malkin, A. Y. *Dokl. Akad. Nauk SSSR* **1973**, *208*, 892.
134. Begishev, V. P.; Volpert, V. A.; Davtyan, S. P.; Malkin, A. Y. *Dokl. Phys. Chem.* **1985**, *279*, 1075–1077.
135. Pojman, J. A.; Ilyashenko, V. M.; Khan, A. M. *Physica D* **1995**, *84*, 260–268.
136. Ilyashenko, V. M.; Pojman, J. A. *Chaos* **1998**, *8*, 285–287.
137. Solov'yov, S. E.; Ilyashenko, V. M.; Pojman, J. A. *Chaos* **1997**, *7*, 331–340.
138. Shult, D. A.; Volpert, V. A. *Int. J. SHS* **1999**, *8*, 417–440.
139. Spade, C. A.; Volpert, V. A. *Combust. Theory Model.* **2001**, *5*, 21–39.
140. Gross, L. K.; Volpert, V. A. *Stud. Appl. Math.* **2003**, *110*, 351–376.
141. Commissioning, D. M. G.; Gross, L. K.; Volpert, V. A. In *Nonlinear Dynamics in Polymeric Systems*; Pojman, J. A.; Tran-Cong-Miyata, Q., Eds.; ACS Symposium Series No. 869; American Chemical Society: Washington, DC, 2003; pp 147–159.
142. Shkadinsky, K. G.; Khaikin, B. I.; Merzhanov, A. G. *Combust. Explos. Shock Waves* **1971**, *7*, 15–22.
143. Masere, J.; Pojman, J. A. *J. Chem. Soc. Faraday Trans.* **1998**, *94*, 919–922.
144. Masere, J.; Stewart, F.; Meehan, T.; Pojman, J. A. *Chaos* **1999**, *9*, 315–322.
145. Tryson, G. R.; Shultz, A. R. *J. Polym. Sci. Polym. Phys. Ed.* **1979**, *17*, 2059–2075.
146. Gray, K. N. Master's Thesis, University of Southern Mississippi, 1988.
147. Manz, B.; Masere, J.; Pojman, J. A.; Volke, F. J. *Polym. Sci. Part A: Polym. Chem.* **2001**, *39*, 1075–1080.
148. Pojman, J. A.; Masere, J.; Petretto, E.; et al. *Chaos* **2002**, *12*, 56–65.
149. Huh, D. S.; Kim, H. S. *Polym. Int.* **2003**, *52*, 1900–1904.
150. Volpert, V. A.; Volpert, V. A.; Pojman, J. A. *Chem. Eng. Sci.* **1994**, *14*, 2385–2388.
151. McFarland, B.; Popwell, S.; Pojman, J. A. *Macromolecules* **2004**, *37*, 6670–6672.
152. McFarland, B.; Popwell, S.; Pojman, J. A. *Macromolecules* **2006**, *39*, 53–63.
153. Binici, B.; Fortenberry, D. I.; Leard, K. C.; et al. *J. Polym. Sci. Part A: Polym. Chem.* **2006**, *44*, 1387–1395.
154. Nason, C.; Pojman, J. A.; Hoyle, C. J. *Polym. Sci. Part A: Polym. Chem.* **2008**, *46*, 8091–8096.
155. Pojman, J. A.; Viner, V.; Binici, B.; et al. *Chaos* **2007**, *17*, 033125.
156. Viner, V. G.; Pojman, J. A.; Golovaty, D. *Physica D* **2010**, *239*, 838–847.
157. Perry, M. F.; Volpert, V. A.; Lewis, L. L.; et al. *Macromol. Theory Simul.* **2003**, *12*, 276–286.
158. Hoyle, C. E.; Lee, T. Y.; Roper, T. J. *Polym. Sci. Part A: Polym. Chem.* **2004**, *52*, 5301–5338.
159. Okay, O.; Bowman, C. N. *Macromol. Theory Simul.* **2005**, *14*, 267–277.
160. Pojman, J. A.; Varisli, B.; Perryman, A.; et al. *Macromolecules* **2004**, *37*, 691–693.
161. Devadoss, D. E.; Pojman, J. A.; Volpert, V. A. *Chem. Eng. Sci.* **2006**, *61*, 1257–1271.
162. Bidali, S.; Fiori, S.; Malucelli, G.; Mariani, A. *e-Polymers* **2003**, *060*, 1–12.
163. Mariani, A.; Fiori, S.; Chekanov, Y.; Pojman, J. A. *Macromolecules* **2001**, *34*, 6539–6541.
164. Fiori, S.; Mariani, A.; Ricco, L.; Russo, S. *Macromolecules* **2003**, *36*, 2674–2679.
165. Mariani, A.; Bidali, S.; Fiori, S.; et al. *e-Polymers* **2003**, *044*, 1–9.
166. Texter, J.; Ziemer, P. *Macromolecules* **2004**, *37*, 5841–5843.
167. Chen, S.; Tian, Y.; Chen, L.; Hu, T. *Chem. Mater.* **2006**, *18*, 2159–2163.
168. Hu, T.; Chen, S.; Tian, Y.; et al. *J. Polym. Sci. Part A: Polym. Chem.* **2006**, *44*, 3018–3024.
169. Mariani, A.; Fiori, S.; Bidali, S.; et al. *J. Polym. Sci. Part A: Polym. Chem.* **2008**, *46*, 3344–3352.
170. Arutiunian, K. A.; Davtyan, S. P.; Rozenberg, B. A.; Enikolopyan, N. S. *Dokl. Akad. Nauk SSSR* **1975**, *223*, 657–660.
171. Chekanov, Y.; Arrington, D.; Brust, G.; Pojman, J. A. *J. Appl. Polym. Sci.* **1997**, *66*, 1209–1216.
172. Frulloni, E.; Salinas, M. M.; Torre, L.; et al. *J. Appl. Polym. Sci.* **2005**, *96*, 1756–1766.
173. Mariani, A.; Bidali, S.; Fiori, S.; et al. *J. Polym. Sci. Part A: Polym. Chem.* **2004**, *42*, 2066–2072.
174. Scognamiglio, S.; Bounds, C.; Luger, M.; et al. *J. Polym. Sci. Part A: Polym. Chem.* **2010**, *48*, 2000–2005.
175. Pojman, J. A.; Elcan, W.; Khan, A. M.; Mathias, L. J. *Polym. Sci. Part A: Polym. Chem.* **1997**, *35*, 227–230.
176. Pojman, J. A.; Griffith, J.; Nichols, H. A. *e-Polymers* **2004**, *13*, 1–7.
177. Dixon, G. D. U.S. Patent 4,222,835, 1980.
178. Scranton, A. B.; Rangarajan, B.; Coons, L. S. U.S. Patent 5,855,837, 1999.
179. Pojman, J. A.; McCordle, T. W. U.S. Patent 6,313,237, 2001.
180. Pojman, J. A.; McCordle, T. W. U.S. Patent 6,057,406, 2000.
181. Chekanov, Y. A.; Pojman, J. A. *J. Appl. Polym. Sci.* **2000**, *78*, 2398–2404.
182. Pfeil, A.; Bürgel, T.; Morbidelli, M.; Rosell, A. U.S. Patent 6,533,503, 2003.
183. Bürgel, T.; Böck, M. U.S. Patent 6,815,517, 2004.
184. Gregory, S. U.S. Patent 6,245,827, 2001.

185. Crivello, J. V. *J. Polym. Sci. Part A: Polym. Chem.* **2007**, *45*, 4331–4340.
186. Pojman, J. A.; McFarland, B.; Popwell, S. US Patent pending.
187. Pojman, J. A.; Fortenberry, D.; Lewis, L. L.; *et al.*; ACS Symp. Ser. (Solvent-Free Polymerization and Processes), *Solvent-Free Synthesis by Free-Radical Frontal Polymerization*; Vol. 713; American Chemical Society: Washington, DC, 1998; 140–153.
188. Hu, T.; Chen, S.; Tian, Y.; *et al.* *J. Polym. Sci. Part A: Polym. Chem.* **2007**, *45*, 873–881.
189. Cai, X.; Chen, S.; Chen, L. *J. Polym. Sci. Part A: Polym. Chem.* **2008**, *46*, 2177–2185.
190. Chen, S.; Hu, T.; Yu, H.; *et al.* *J. Polym. Sci. Part A: Polym. Chem.* **2007**, *45*, 4322–4330.
191. Washington, R. P.; Steinbock, O. *J. Am. Chem. Soc.* **2001**, *123*, 7933–7934.
192. Lu, G. D.; Yan, Q. Z.; Ge, C. C. *Polym. Int.* **2007**, *56*, 1016–1020.
193. Pujari, N. S.; Vishwakarma, A. R.; Pathak, T. S.; *et al.* *Polym. Int.* **2004**, *53*, 2045–2050.
194. Tu, J.; Chen, L.; Fang, Y.; *et al.* *J. Polym. Sci. Part A: Polym. Chem.* **2010**, *48*, 823–831.
195. Fang, Y.; Yu, H.; Chen, L.; Chen, S. *Chem. Mater.* **2009**, *21*, 4711–4718.
196. Feng, Q.; Yan, Q.-z.; Ge, C.-c. *Chin. J. Polym. Sci.* **2009**, *27*, 747–753.
197. Yan, Q. Z.; Su, X. T.; Zhang, W. F.; Ge, C. C. *Chem. J. Chin. Univ.* **2005**, *26*, 1363–1365.
198. Yan, Q.-Z.; Zhang, W.-F.; Lu, G.-D.; *et al.* *Chem. Eur. J.* **2005**, *11*, 6609–6615.
199. Yan, Q.; Zhang, W. F.; Lu, G. D.; *et al.* *Chem. Eur. J.* **2006**, *12*, 3303–3309.
200. Scognamiglio, S.; Alzari, V.; Nuvoli, D.; *et al.* *J. Polym. Sci. Part A: Polym. Chem.* **2011**, n/a-n/a.
201. Proietti, N.; Capitani, D.; Cozzolino, S.; *et al.* *J. Phys. Chem. B* **2006**, *110*, 23719–23728.
202. Mariani, A.; Bidali, S.; Cappelletti, P.; *et al.* *e-Polymers* **2006**.
203. Vicini, S.; Mariani, A.; Princi, E.; *et al.* *Polym. Adv. Technol.* **2005**, *16*, 293–298.
204. Kim, C.; Teng, H.; Tucker, C. L.; White, S. R. *J. Comp. Mater.* **1995**, *29*, 1222–1253.
205. White, S. R.; Kim, C. *J. Reinf. Plast. Compos.* **1993**, *12*, 520–535.

**Biographical Sketch**

John A. Pojman is a professor in the Macromolecular Science Division of the Department of Chemistry at Louisiana State University. He earned his doctorate in chemical physics from the University of Texas at Austin. Dr. Pojman was a faculty member at the University of Southern Mississippi for 18 years. He has published over 100 peer-reviewed publications and coedited three monographs and coauthored another one. His interests include nonlinear dynamics with polymers, cure-on-demand polymerizations, nonequilibrium thermodynamics of miscible fluids, microgravity research, and the aquatic salamanders of Louisiana. He also claims the world's largest collection of pocket protectors.